Environmental Microbiome

https://doi.org/10.1186/s40793-026-00894-8

Article in Press

Distinct taxonomic signatures in the rhizobiome of two native plants from the polyextreme Salar de Huasco ecosystem

Received: 4 December 2025

Accepted: 1 April 2026

Published online: 13 April 2026

Cite this article as: Castro-Severyn J., Pardo-Esté C., Saraiva J. *et al.* Distinct taxonomic signatures in the rhizobiome of two native plants from the polyextreme Salar de Huasco ecosystem. *Environmental Microbiome* (2026). https://doi.org/10.1186/s40793-026-00894-8

Juan Castro-Severyn, Coral Pardo-Esté, João Saraiva, Jonathan Fortt, Ramona Mörchen, Virginia H. Albarracin, Claudia P. Saavedra, Roland Bol, Eduardo Castro-Nallar, Ulisses Nunes Rocha & Francisco Remonsellez

Distinct Taxonomic Signatures in the Rhizobiome of Two Native Plants from the Polyextreme Salar de Huasco Ecosystem

Juan Castro-Severyn[1,2]*; Coral Pardo-Esté[3]; João Saraiva[4]; Jonathan Fortt[1,5]; Ramona Mörchen[6]; Virginia H. Albarracin[7]; Claudia P Saavedra[8]; Roland Bol[9]; Eduardo Castro-Nallar[10,11,12]; Ulisses Nunes da Rocha[4] and Francisco Remonsellez[1,2]*.

[1] Laboratorio de Microbiología Aplicada y Extremófilos, Facultad de Ingeniería y Ciencias Geológicas, Universidad Católica del Norte. Antofagasta - Chile.

[2] Centro de Investigación Tecnológica del Agua en el Desierto - CEITSAZA, Universidad Católica del Norte, Antofagasta - Chile.

[3] Laboratorio de Ecologia Molecular y Microbiologia Aplicada, Departamento de Ciencias Farmacéuticas, Facultad de Ciencias, Universidad Católica del Norte. Antofagasta - Chile.

[4] Department of Applied Microbial Ecology. Helmholtz Centre for Environmental Research - UFZ. Leipzig - Germany.

[5] Laboratorio de Fisiología Vegetal, Facultad de Ciencias Naturales y Oceanografía, Universidad de Concepción. Concepción, Chile.

[6] Institute of Crop Science and Resource Conservation INRES, Soil Science and Soil Ecology, University of Bonn, Bonn, Germany.

[7] Laboratorio de Microbiología Ultraestructural y Molecular, Centro Integral de Microscopía Electrónica (CIME), CONICET - Universidad Nacional de Tucumán, Tucumán, Argentina.

[8] Laboratorio de Microbiología Molecular. Facultad de Ciencias de la Vida, Universidad Andrés Bello. Santiago - Chile.

[9] Institute of Bio- and Geosciences, Agrosphere (IBG-3), Forschungszentrum Jülich GmbH, Jülich, Germany.

[10] Instituto de Ciencias Biológicas, Universidad de Talca, Campus Talca, Talca, Chile.

[11] Centro de Ecología Integrativa, Universidad de Talca, Talca, Chile.

[12] Cape Horn International Center, Universidad de Magallanes, Teniente Muñoz 166, Puerto Williams 6350000, Chile.

* Correspondence: Juan Castro-Severyn juan.castro02@ucn.cl and Francisco Remonsellez, fremonse@ucn.cl

Running title: Taxonomic signatures from native plants rhizobiomes thriving in the Chilean altiplano.

ABSTRACT

Background: Global food security faces mounting pressure from population growth, climate change, and deteriorating soil conditions. Rhizospheric microbial communities (rhizobiomes) play a key role in plant physiology, enhancing growth and tolerance to abiotic stress. To explore their potential contribution to plant resilience in extreme environments, we characterized the rhizobiomes of *Deyeuxia curvula* and *Werneria incisa* across the Salar de Huasco (SH) in the Chilean Altiplano (~3800 masl), a polyextreme ecosystem characterized by high UV radiation, salinity gradients, water scarcity, and high metal concentrations. Our objectives were to identify microbial taxa associated with plant adaptation and to infer functional traits linked to survival under these conditions.

Results: We generated 16S rRNA amplicon sequencing data from 200 rhizosphere samples. Both host plant identity and geographic location significantly shaped microbial community composition, with site explaining a larger proportion of variance than plant identity alone. Actinomycetota dominated both rhizobiomes, with genera such as *Modestobacter* and *Blastococcus* — known for UV resistance, desiccation tolerance, and genomic plasticity — contributing to species-specific profiles. At the genus level, *Ilumatobacter*, *Nesterenkonia*, *Tropicimonas*, and *Nitriliruptor* were enriched in *D. curvula*, whereas *Pseudarthrobacter*, *Kocuria*, *Crossiella*, and *Blastococcus* were more abundant in *W. incisa*. Network analysis revealed greater complexity and functional redundancy in *D. curvula*, while *W. incisa* harbored a more generalist network. Functional predictions indicated that chemoheterotrophy dominates both rhizobiomes, while denitrification, methylotrophy,

and ureolysis were enriched in *W. incisa*, and osmotic stress-tolerance functions such as glycine betaine cycling were enriched in *D. curvula*.

Conclusion: The two plants follow contrasting ecological strategies: *D. curvula* relies on a specialization and resilience strategy supported by a diverse, stress-adapted rhizobiome, while *W. incisa* employs a nutritional versatility strategy through a generalist, metabolically flexible community. These findings highlight the value of high-altitude Andean rhizobiomes as reservoirs of great biodiversity with relevant functions for future biotechnological applications particularly for agriculture under arid and saline conditions. This underscores the importance of extending conservation policies to native microbial communities in protected areas such as the Salar de Huasco.

KEY WORDS: Rhizobiomes, *Deyeuxia curvula*, *Werneria incisa*, Salar de Huasco, abiotic stress.

BACKGROUND

Global food security faces an unprecedented challenge due to rapid population growth, accelerated climate change, and declining soil quality. Significant limitations to increasing or maintaining crop yields include their vulnerability to rising temperatures and water shortages [1]. 4/6/2026 2:14:00 PMBiotechnology offers information and strategies to enhance crops and agricultural practices [2,3]. Extreme environments serve as natural laboratories that help us understand the limits of life and the mechanisms by which organisms survive various stressors. Northern Chile continually experiences drought, soil aridity, and high radiation [4–6]; therefore, it is an attractive and unique natural setting to study the boundaries of life and a source of new or unknown metabolic pathways and molecular mechanisms [7]. Consequently, plants thriving under such conditions can serve as models to improve agriculture, given their functional novelty and resistance to microorganisms [8,9].

Salar de Huasco, located in northern Chile's Tarapacá region, experiences substantial climatic variations, high salinity, high UV radiation, a negative water balance, low atmospheric pressure (3800 masl), and the presence of toxic compounds such as arsenic [10–12]. This ecosystem is characterized by high microbial diversity and richness, driven by various stressors and spatial stratification, such as the salinity gradient from north to south [13,14]. Microbial communities inhabiting Salar de Huasco include UV- and arsenic-resistant bacteria and strains capable of producing potential drugs [11,12,15]. The plant coverage in SH, which is less than 10% over 78% of the area and more than 10% in the remaining 22%, is mainly made up of perennial herbaceous species like *Festuca nardifolia*, *Festuca deserticola*, *Puccinellia frigida*, *Deyeuxia curvula*, *Carex misera*, *Werneria incisa*, *Frankenia triandra*, and *Pratia repens*. This vegetation mainly consists of saline grasslands, with some wetlands—such as *Oxychloe andina, Zameioscirpus atacamensis,* and *Deyeuxia curvula*—as reported in an inventory by the Chilean Ministry of Agriculture's "Servicio Agrícola y Ganadero (SAG)."

D. curvula and *W. incisa* are the most common plants and have greater coverage in the Salar de Huasco. Furthermore, these species are the only ones found both alone and as part of species assemblages. Other plant species in the area have been studied, such as *Carex misera,* which serves as a typical model for high-altitude vegetation and genetic population studies. Additionally, *Werneria incisa* has been studied to produce metabolites (terpenoids, benzofurans, benzopyrans, flavonoids, leucoanthocyanidins, catechins, saponins, and alkaloids). Conversely, *Deyeuxia curvula* is of archaeological interest and is vital for the dietary needs of llamas and alpacas. Finally, *Puccinellia frigida* can resist and accumulate boron, demonstrating potential for bioremediation. [16–20]. However, there are no studies on the microbiome and its interaction with native plants, which, due to environmental pressures, are considered essential models for understanding the basis of abiotic stress resistance and resilience.

The rhizosphere is the zone where plant roots touch soil, allowing many beneficial interactions between plants and microorganisms. [21,22]. Plant phenotype is the overall outcome of their genotype, environment, and microbiome [23]. The study of the plant microbiome is relatively new and has shown that microbes in the rhizosphere (rhizobiome) significantly affect plant health and growth, as these interactions can improve nutrient availability [22,24–26]. Extreme conditions appear to enhance these mutualistic relationships by compensating for metabolic deficiencies [27].

Microorganisms are crucial for sustaining ecosystem health and biochemical cycles. Specifically, they can enhance plants with advantageous traits [26]. However, the mechanisms and dynamics of rhizobiomes and their effects on plant fitness remain poorly understood, especially in extreme environments where taxonomic and metabolic diversity are significant.

Microbial symbionts can improve plant colonization and survival, regardless of the plants' innate traits [26,28]. For example, fungi and bacteria isolated from extremophile plant roots can boost drought resistance, enhance photosynthesis rates, and increase biomass [29,30]. These traits can be transferred to other crop-related plants, such as *Lactuca sativa*, *Hordeum vulgare*, and *Oryza sativa* [31–34]. Specific functions attributed to microorganisms include producing phytohormones and exhibiting ACC deaminase activity, which reduces harmful ethylene buildup caused by stress. They also contribute to salt tolerance and the solubilization of zinc, potassium, and phosphorus; nitrate reduction and fixation; and the production of siderophores and secondary metabolites [9,35–39]. These functions align with observations that no functional differences are found between rhizobiomes, even when their taxonomic makeup varies widely [40,41].

Evidence suggests that poly-extreme bacteria can enhance plant resistance to abiotic stresses. For example, a halotolerant bacterium classified as *Exiguobacterium*, isolated from the Chilean Altiplano [42,43], has been shown to promote plant growth under salinity stress

[44,45]. However, rhizospheric interactions in these extreme environments are not well understood, as multiple stressors co-occur and influence the functions of biotic entities.

Previous characterizations of microbial potential depended on accessible sequencing technologies to investigate biology and beneficial interactions. [46], and facilitate global research on microbial abundance, composition, and community functions. By examining areas around the plant—such as bare soil, bulk soil, rhizosphere, and rhizoplane—we seek to identify differences that indicate functional relationships. There is also a transition from bulk soil to the rhizoplane that filters microbes interacting with the plant [47,48].

This study aims to characterize the microbial community in the rhizospheric fraction and surrounding area, where functional dynamics influence plant physiology in a poly-extreme environment marked by high solar radiation, water scarcity, metals, and other stresses that shape the ecosystem. By examining the soil and plant-associated microbiome, we can estimate the beneficial conditions microbes offer for plant growth and understand how plants recruit specific microorganisms from the available soil diversity, thereby shaping the rhizobiome composition.

MATERIALS AND METHODS

Field trip and sample collection

A sampling expedition was carried out in August 2021 at Salar de Huasco National Park, located on the Chilean Altiplano. Nine sampling sites were established around the Salar basin (H0 – H8), along with a control site 5 km outside the basin where specimens of *D. curvula* and *W. incisa* were also found (Figure 1). At each site, five specimens of each plant species were randomly selected within a 50x50 m area, choosing plants of similar size (~40 cm). The plants were placed in sterile bags and stored in a container, then kept in a -20°C freezer until transported to the laboratory for analysis. Moreover, rhizospheric soil samples were collected from the soil that remained loosely attached to the roots once we completely dug out the plant. These samples were stored in sterile sampling bags and kept

in the container. Some physicochemical parameters, including temperature, salinity, and pH, were measured *in the* field with field testers (HI98192 and HI981045, HANNA Instruments). Rhizoplane samples were obtained in the laboratory by scraping off the material attached to the plants roots (after shaking the plant) with a sterile spatula, this was carried out for each of the 100 collected plants inside a laminar flow cabinet, which was then collected in sterile tubes for further processing. The sampling design was fully balanced, with exactly five specimens of each plant species collected at each of the ten sampling sites (5 plants × 2 species × 10 sites = 100 plants), yielding 100 rhizospheric soil samples and 100 rhizoplane samples for a total of 200 samples.

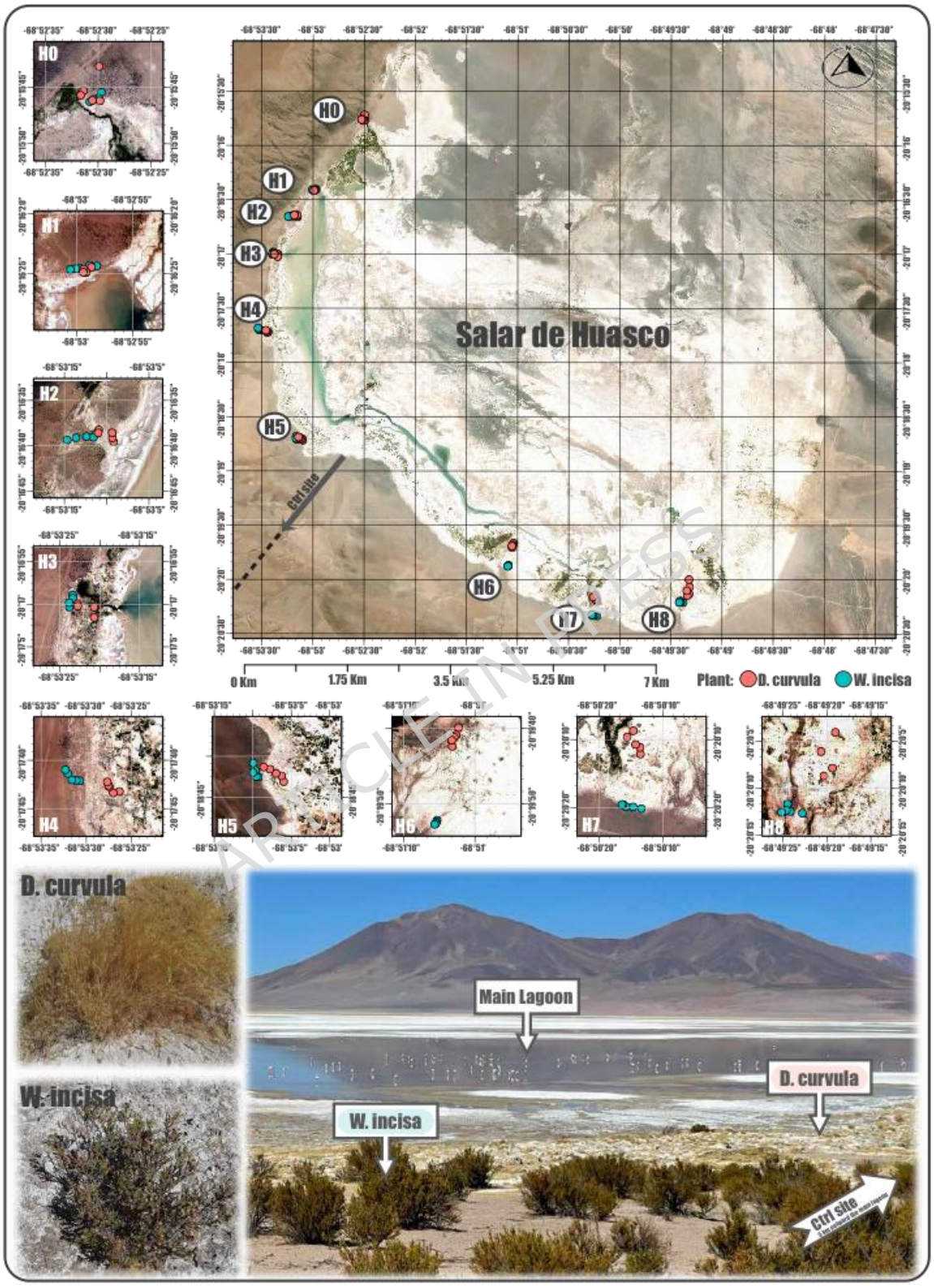

Figure 1. **Salar de Huasco study area.** Top panel: SH map (68°47' - 68°54' W and 20°15' - 20°20' S Source: Google Earth) showing the ten sampled sites, also the localization and distribution of the sampled plants

(Coordinates in Supplementary Table S1). Bottom left panel: photographs of the two studied plant species. Bottom right panel: picture of the SH landscape, where the studied species distribution can be observed.

Soil edaphic parameters

These measurements were taken from 100 rhizospheric soil samples. Soil moisture was determined by measuring the weight loss after drying the samples at 105°C for 48 hours. Additionally, these dried samples were used to measure pH and electrical conductivity (EC) by preparing a soil-distilled water suspension in a 1:2.5 ratio, which was then analyzed with benchtop pH and conductivity meters (HI2020 and HI2030, HANNA Instruments). Furthermore, the percentage of total organic matter (OM) was determined using the weight loss method after calcining 50 g of soil at 560°C for 8 hours. The contents of total N and C were measured in an elemental analyzer (Vario MICRO Cube, Elementar) following the ISO 10694, 1995 standard, using 20 mg of soil. Lastly, the concentrations of As, B, Ca, Cd, Cu, Fe, K, Li, Mg, Mn, Mo, and Zn were measured by ICP-OES (inductively coupled plasma optical emission spectrometry) (Optima™ 7000 DV, PerkinElmer®) after acid digestion of 300 mg of soil.

DNA Extraction and Amplicon Sequencing

Total DNA was extracted from the 100 rhizospheric soil and the 100 rhizoplane samples using the E.Z.N.A. Soil DNA Extraction Kit (Omega Bio-tek, USA) following the manufacturer's instructions with 0.25 g of material. DNA integrity, quality, and quantity were verified by 1% agarose gel electrophoresis, 260/280 ratio spectroscopy, and fluorescence measurements using a Qubit 3.0 fluorometer along with the Qubit dsDNA HS assay kit (Thermo Fisher Scientific, USA). To monitor potential contamination during DNA extraction and PCR amplification, extraction blanks were included in each extraction batch. These controls consisted of molecular-grade water processed alongside samples using the same reagents, consumables, and laboratory environment. All extraction blanks were quantified using the same fluorometric assay applied to samples and were consistently below the limit of detection. Also, these controls were subsequently subjected to 16S rRNA gene PCR amplification using the 27F and 1525R primers to discard the presence of DNA

contamination, which was confirmed by the absent of visible amplicons in agarose gel electrophoresis for all extraction blanks, whereas successful amplification was observed for all biological samples. Subsequently, the DNA samples were sent to the Helmholtz Centre for Environmental Research (Leipzig, Germany) for the library construction, amplicon sequencing of the bacterial 16S rRNA gene, targeting the V3–V4 hypervariable region with the 341F and 785R primers [49] and the sequencing run on an MiSeq platform (Illumina Inc.).

Determination of amplicon sequence variants (ASVs)

This analysis was conducted using R v4.2.2 and RStudio v2023.12.0+369, following the DADA2 v1.26.0 R package pipeline [50] to identify amplicon sequence variants (ASVs) in each sample. Briefly, the reads were quality-checked and then trimmed (truncLen = c(270, 190), maxN = 0, maxEE = c(2, 2), truncQ = 2, and rm.phix = TRUE), followed by dereplication, denoising, and merging of paired reads. Next, the ASV table was created, allowing up to 2 expected errors. Chimeras were removed, and taxonomic classification was performed using the Silva v138 database [51] with the naive Bayesian classifier [52]. ASVs classified as Eukarya, Chloroplast, and Mitochondria were then filtered out. Additionally, a multi-sequence alignment was generated with DECIPHER v2.26.0 [53] to infer phylogeny, and the resulting tree was inferred using FastTree v2.1.11 [54]. Furthermore, a phyloseq object containing the ASVs, taxonomy, phylogenetic tree, and sample metadata was created using the R package Phyloseq v1.42.0 [55].

Diversity analysis

Alpha diversity indices (Shannon, Simpson, Chao1 and Faith's Phylogenetic diversity) were computed with the raw ASV counts using the Microbiome v1.20.0 and Btools v0.0.1 R packages. To compare soil types, plant species, and sites, the Wilcoxon test ($P < 0.05$) was employed to identify statistical significance, and visualizations were created with the ggpubr v0.6.0 R package. For beta diversity the ASV counts were normalized through variance-stabilizing transformation with the R package DESeq2 v1.38.3 [56] and these were

analyzed using Jensen–Shannon Divergence metric as distance with Principal Coordinates Analysis (PCoA) through the ampvis2 v2.4.5 R package [57]. Sample dissimilarity by site was evaluated with hierarchical clustering using Hellinger-transformed Bray-Curtis distances, as implemented in the MicrobiotaProcess v1.2.2 R package [58]. Both distance metrics were selected based on their complementary properties (Bray–Curtis focuses on abundance differences, while Jensen–Shannon divergence compares full probability distributions), to assess the robustness of the observed biological patterns. Also, to formally partition the variance in microbial community composition PERMANOVA analyses were performed using the adonis2 function from the vegan R package, with 999 permutations. All statistical analyses were conducted both including and excluding the control site (located 5 km outside the SH basin) to assess the robustness of the results; unless otherwise stated, only results excluding the control site are presented.

Taxonomy composition

Taxonomy at the phylum, family, and genus levels as relative abundance were visualized using the ggplot2 v3.4.1, fantaxtic v0.2.0, and ampvis2 v2.7.35 [57] R packages. Additionally, we identified the ASVs most likely explaining the differences between the two plant species using LEfSe (Linear Discriminant Analysis Effect Size) [59] in the microbial v0.0.21 R package.

Co-occurrence networks analysis

Co-occurrence networks were created by agglomerating the phyloseq object at the lowest available taxonomic rank for each ASV using the microbiomeutilities v1.00.11 R package [60] and transformed as relative abundance. Prior to network inference, taxa were filtered to remove rare taxa and reduce spurious correlations. Only taxa present in at least one sample with a minimum relative abundance of 0.5% were retained, using the kOverA function (k = 1, A = 0.005) from the genefilter R package. The network was estimated with the SpiecEasi v0.1.4 [61] R package using the Meinshausen-Bühlmann neighborhood selection method (method = 'mb'). Model selection was performed using the StARS (Stability Approach to Regularization Selection) criterion with a stability threshold of 0.05,

50 subsampling repetitions (rep.num = 50), a regularization path of 20 lambda values (nlambda = 20), and a minimum lambda ratio of 1×10^{-2} (lambda.min.ratio = 1e-2). Networks were visualized using the GGally v1.5.0 [62] R package. Keystone taxa were identified based on two complementary network centrality metrics calculated using the igraph R package: degree centrality, defined as the number of direct connections of a given node, and betweenness centrality, defined as the number of shortest paths between all pairs of nodes that pass through a given node. Taxa were classified as keystones if they simultaneously exceeded a degree threshold of > 2.5 and a betweenness centrality threshold of > 50 for *D. curvula*, and > 2 and > 13 for *W. incisa*, thresholds determined empirically by inspecting the distribution of each metric within each network.

Core microbiome analysis

The same phyloseq object (agglomerated to the lowest available taxonomic rank) was used to identify the core ASVs and compare them between both plant species using the ampvis2 v2.7.35 [57] R package. The core microbiome was defined as taxa present in at least 80% of samples, a prevalence threshold widely applied in microbiome studies. Core taxa were reported at the lowest available taxonomic rank for each ASV, as many members of these underexplored and extreme environments lack genus-level classification in current reference databases.

Environmental variables correlation

To evaluate the influence of environmental variables on community composition and distribution, redundancy analysis (RDA) was performed on Hellinger-transformed ASV abundance data using the amp_ordinate function from the ampvis2 (v2.4.5) R package [57]. The ordination was constrained by plant species and site as explanatory variables. The overall significance of the constrained ordination model was assessed using permutation-based ANOVA (anova.cca, 999 permutations) from the vegan R package. Environmental variables were subsequently fitted post-hoc onto the ordination using the envfit function from the vegan R package (999 permutations), and only statistically significant vectors ($p <$

0.05) were displayed. Spearman's rank correlation coefficients between the most abundant genera and key abiotic variables were calculated using the taxa.env.correlation function from the microbiomeSeq R package [63]. Multiple testing correction was applied using the Benjamini-Hochberg (BH) false discovery rate method.

Functional inference

Estimated functional potential signatures and metabolic pathway abundances based on the abundance and taxonomic affiliations of identified ASVs using PICRUSt2 v2.4.1 software [64] through the Kyoto Encyclopedia of Genes and Genomes (KEGG) [65] and MetaCyc [66] pathway databases. Differential abundance among pathways was determined using the Kruskal-Wallis test ($p \leq 0.05$) and the Benjamini-Hochberg correction for false discovery rate with the ggpicrust2 v1.7.2 R package [67]. Additionally, we assessed ecologically relevant functions by querying the Functional Annotation of Prokaryotic Taxa (FAPROTAX) database v1.2.7 [68] with the identified taxa.

Data availability

The whole amplicon sequencing raw data sets have been deposited at DDBJ/ENA/GenBank under the Bioproject: PRJNA1230159.

RESULTS

Amplicon sequencing of the 16S rRNA gene was performed to characterize the microbial communities associated with the roots of *W. incisa* and *D. curvula* growing in the Salar de Huasco basin. A total of 200 samples (100 from plant roots and 100 from rhizospheric soils) were collected from 10 different sites (H0 to H8 and a control site) during the winter season (August) of 2021. While in the field, we observed an interesting pattern in the plant distribution along the SH. At the western sites (H0), both species were found growing intermixed; however, as we moved eastward, the species gradually separated until they were found growing completely separately at the easternmost site (H8) (Figure 1).

To compare the diversity of rhizospheric communities from plants thriving in the SH, we conducted a distance-based analysis using the Jensen–Shannon Divergence metric. The results showed a clustering pattern between the two plant species, with noticeable overlap in communities from the westernmost sites of the SH. However, as we moved eastward, a clear separation appeared between the rhizospheric communities of the two species (Figure 2A), reflecting their spatial distribution. Hierarchical clustering of samples by "site" further supports this trend (Figure 2B), with all samples from the western sites (H0 to H4) forming a distinct cluster, clearly separated from those in the eastern sites (H5 to H8). Additionally, we evaluated four different alpha diversity indices to determine whether the communities were comparable in terms of composition and species distribution across both plant species (*D. curvula* and *W. incisa*), soil compartments (rhizosphere and rhizoplane), and locations (H0 to H8). The results indicated that, despite some overlap, significant differences exist between the communities (Figure 2C). All indices showed a consistent pattern, with *D. curvula* communities exhibiting greater richness, diversity, and evenness (Chao1, PD, and Shannon), and lower dominance (Simpson) compared *to W. incisa* communities.

There are no significant differences in richness and diversity among the soil compartments for each plant (Figure 2D), which aligns with the PCoA analysis showing samples from both soil compartments intermixed (circles and triangles in Figure 2A). However, significant differences were observed across locations, especially within the *D. curvula* communities, which exhibited greater variability. Notably, site H4 showed significant differences for all indices compared to most other sites (Supplementary Figure S1). In contrast, site H2 demonstrated the highest number of significant differences among the *W. incisa* communities.

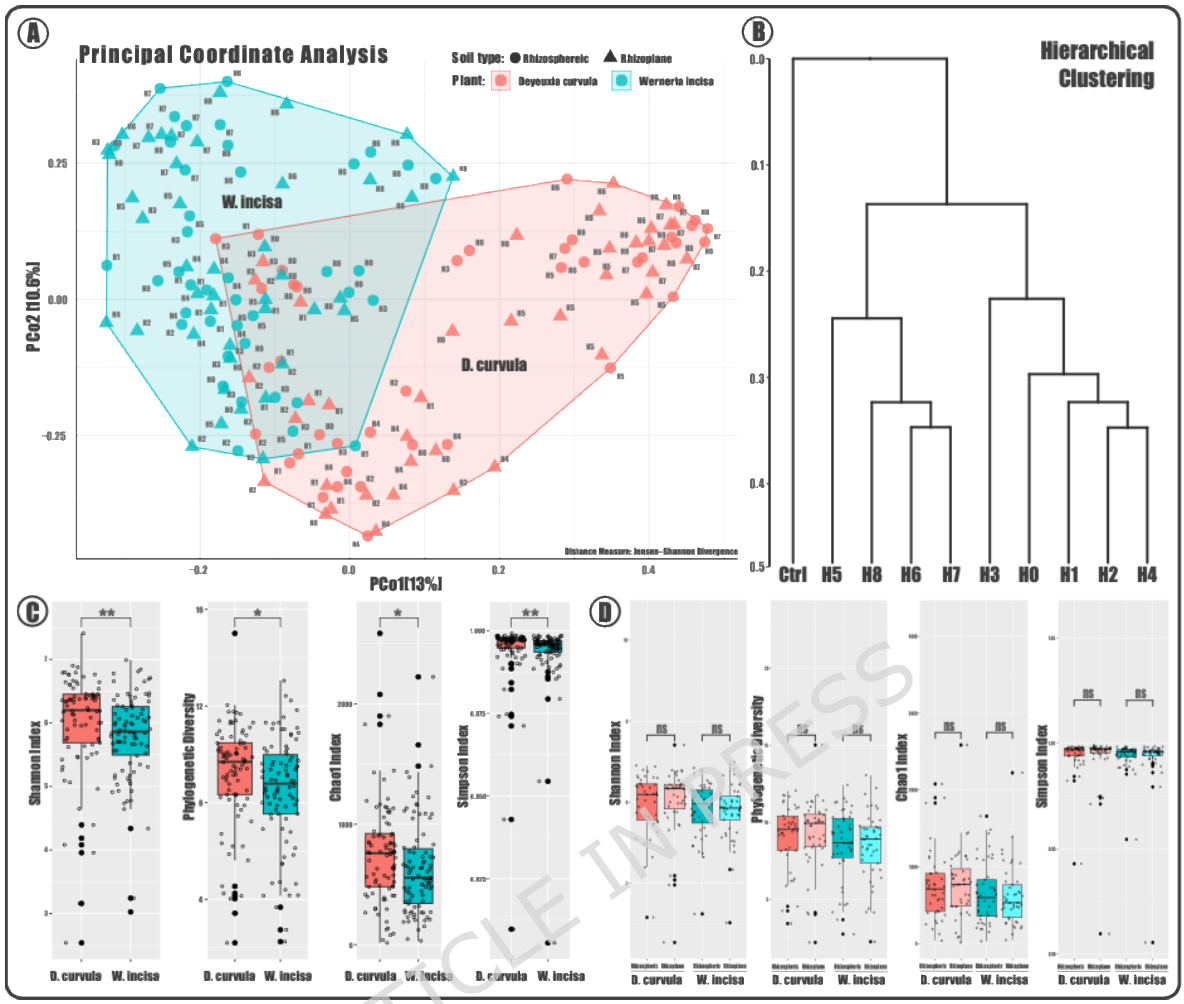

Figure 2. **Bacterial community diversity among SH plant species and sites.** A) Principal coordinate analysis (PCoA) with the ASVs' relative abundance using Jensen–Shannon Divergence as distance metric; each point corresponds to a community, tagged by site, colored by plant species, and shaped by soil type; PCo1 and PCo2 explained 13% and 10.6% of the total variance, respectively. B) Hierarchical clustering of all studied sites, according to their diversity patterns (considering all *D. curvula* samples) by Hellinger transformed Bray-Curtis distances. C) Comparison of alpha diversity indices for all studied samples among plant species and D) soil types for each plant species. Statistical significance according to the Mann–Whitney–Wilcoxon test (* $p < 0.05$; ** $p < 0.01$).

We also performed a principal coordinates analysis for each plant to evaluate sample dispersion across different locations (Figure 3). The results indicate greater dispersion among the *D. curvula* samples and the formation of two distinct groups (H0-H4 and H5-H8). This pattern was not seen in the *W. incisa* samples, where no clear clusters appeared, and

there was more overlap. Notably, although the control samples for both plants were completely separated, the separation was more evident in *D. curvula*, which also formed a tighter cluster.

PERMANOVA analyses revealed that both plant species ($F = 13.88$, $R^2 = 0.079$, $p < 0.001$) and geographic site ($F = 3.62$, $R^2 = 0.159$, $p < 0.001$) were significant independent drivers of community composition, with site explaining a larger proportion of variance than plant identity alone. The plant species/site interaction was also significant ($F = 4.41$, $R^2 = 0.159$, $p < 0.001$), indicating that the effect of plant identity on rhizobiome composition varies across sampling locations. Within-plant analyses further confirmed that site significantly structured communities in both *D. curvula* ($R^2 = 0.374$, $p < 0.001$) and *W. incisa* ($R^2 = 0.302$, $p < 0.001$), with *D. curvula* showing greater sensitivity to geographic location consistent with its stronger north-to-south structuring pattern. Moreover, this analysis was also performed to compare soil types and confirmed that there are no differences between rhizospheric soil and rhizoplane ($F = 0.71$, $R^2 = 0.004$, $p = 0.93$). Also, results were consistent whether or not the control site was included in the analyses (including control site: plant species $F = 11.89$, $R^2 = 0.062$, $p < 0.001$ and geographical site $F = 4.91$, $R^2 = 0.206$, $p < 0.001$), confirming the robustness of the observed patterns independent of the inclusion of the control site.

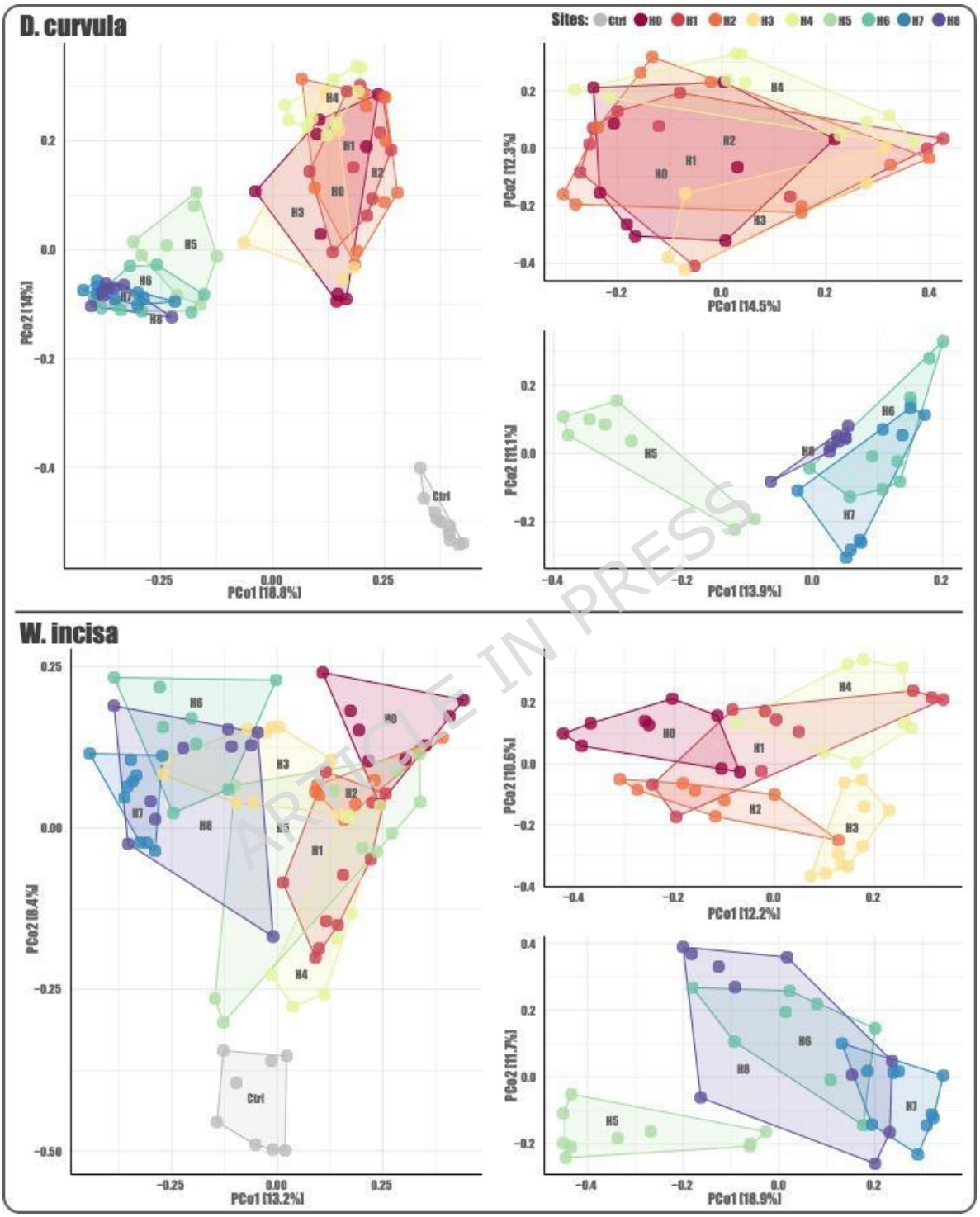

Figure 3. **Ordination of bacterial communities for both plant species according to the studied sites.** Beta diversity analysis by Principal Coordinates Analysis (PCoA) on ASVs relative abundance using Jensen–Shannon Divergence as distance metric, to indicate the similarity level to all other samples. Each point corresponds to a community colored by site. For both plant species (*D. curvula* at the top panel and *W. incisa* at the bottom

panel): the communities of all the studied sites are shown on the left, the subsets of communities for the sites H0 to H4 on the top-right, and for the sites H5 to H8 on the bottom-right.

Since no significant differences were detected between soil compartments (rhizoplane vs. rhizosphere) in either plant species, this distinction was not considered in subsequent analyses, which from this point on were focused on plant species and sampling locations. We observed a clear dominance of the Actinomycetota phylum in both plants across all locations, ranging from 53% to 68% in *D. curvula* and 52% to 76% in *W. incisa*. At the control site, Actinomycetota dominance was even higher, reaching 95% for *D. curvula* and *91% for W. incisa* (Figure 4A). Pseudomonadota was the second most abundant phylum in both plant species, with a higher proportion in *D. curvula* (15% to 36%). Additionally, the Chloroflexi and Deinococcota phyla were notably abundant, with Deinococcota present only at the SH western sites (H0 to H4 for *D. curvula* and H0 to H5 for *W. incisa*). In contrast, the Candidatus Entotheonellaeota phylum was mainly enriched in the eastern locations of the SH. There was also a low abundance of Cyanobacteriota and Bacillota, which generally account for less than 1% of the community, especially in *W. incisa*, where these phyla are even less abundant compared to *D. curvula*.

To gain deeper insights into the communities and further distinguish between the two plant species and the studied locations, we analyzed the taxonomic composition at the family level (Figure 4B). One of the most noticeable findings is the high abundance of the Micrococcaceae family, especially in communities associated with *W. incisa*, where it makes up an average of 28.5% across all locations. In contrast, this family is the second most abundant in *D. curvula* communities, with an average of 11.8%, but its abundance drops notably in the localities at the SH east (H4-H8). For *D. curvula*, the most abundant family is Euzebyaceae, with an average of 14.9% across locations. This family also shows a decreasing trend at the eastern sites of the SH, a pattern seen in several other families linked to *D. curvula*, including Trueperaceae, Microbacteriaceae, Propionibacteriaceae, Pseudonocardiaceae, and Intrasporangiaceae. Conversely, families such as Rhodomicrobiaceae, Entotheonellaceae, Geminicoccaceae, Ilumatobacteraceae, and

Sphingomonadaceae are more enriched in these eastern locations. In the case of *W. incisa*, Euzebyaceae and Geodermatophilaceae are the second and third most common families, with average proportions of 6.5% and 5.9%, respectively. The patterns for *W. incisa* are more consistent across the east and west locations of the SH, with less noticeable differences. However, families like Nitriliruptoraceae, Microbacteriaceae, Trueperaceae, Intrasporangiaceae, and Propionibacteriaceae are more prevalent in the western sites, while Rhodomicrobiaceae, Ilumatobacteraceae, and Geminicoccaceae are more dominant in the eastern sites.

The most relevant differences between the studied communities relate to how key families, such as Euzebyaceae, Nitriliruptoraceae, Ilumatobacteraceae, and Sphingomonadaceae, are distributed and how abundant they are. These families are more common in *D. curvula*. Additionally, Micrococcaceae, Geodermatophilaceae, and Pseudonocardiaceae show higher levels in *W. incisa*. Some families are unique to each species: Nostocaceae was found only in *D. curvula*, while Mycobacteriaceae was exclusively present in *W. incisa*. At the control site, the microbial communities of both plants are mainly made up of just four families, which make up 94.5% of the total abundance in *D. curvula* and 90.1% in *W. incisa*. However, differences in the relative abundance of these families are observed between the two plants. In *D. curvula*, Micrococcaceae, Pseudonocardiaceae, Geodermatophilaceae, and Propionibacteriaceae account for 11.2%, 42.7%, 14.4%, and 26.2%, respectively. In *W. incisa*, these same families represent 23.8%, 15.7%, 14.5%, and 36.1% of the total, respectively.

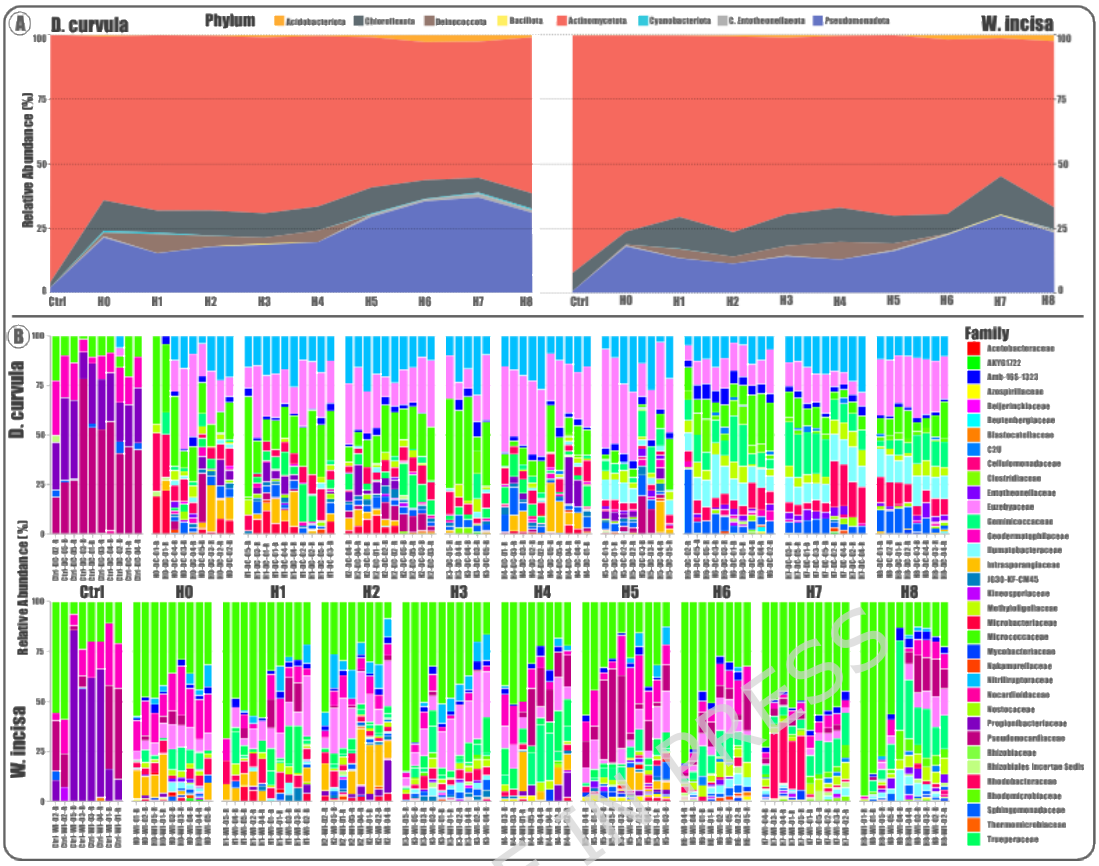

Figure 4. **Bacterial community composition.** A) Relative abundance of taxa phyla throughout the study area for both plant species. B) Relative abundance of families for all the communities of both plant species.

At the genus level, the rhizospheric communities from both plant species showed different patterns across all sampled sites in terms of composition and abundance. The heatmap (Figure 5: left panel) displays the top 25 most ASVs across both plant species and all locations (H0–H8). A clear difference in the relative abundance patterns is seen between the two plant species. Genera such as *Sphingomonas*, *Pseudarthrobacter*, *Kocuria*, *Modestobacter*, and *Blastococcus* were among the most notable, as their abundance and distribution varied between species and sites.

The Linear Discriminant Analysis Effect Size (LEfSe) highlights the genera that are significantly enriched in association with each plant species (Figure 5: right panel). Notably, *Paenarthrobacter*, *Friedmanniella*, and *Roseomonas* show higher LDA scores in *W. incisa*

rhizobiomes, whereas *Nesterenkonia*, *Nitrolancea*, and *Ilumatobacter* are enriched in the rhizobiomes of *D. curvula*. Interestingly, *W. incisa* exhibits a significantly greater abundance of Actinomycetota (*Pseudarthrobacter*, *Modestobacter*, and *Blastococcus*). Moreover, other genera such as *Sphingomonas* and *Mycobacterium* are detected in both rhizobiomes, but with differential abundance and preferential dominance for one of the two.

Regarding differences between sites, the genera *Sphingomonas*, *Mycobacterium*, and *Skermanella* are highly abundant in locations H0 and H1. Two Actinomycetota genera, *Modestobacter* and *Blastococcus,* are enriched in the H2/H3 locations, while *Microlunatus*, *Crossiella*, and *Truepera* are dominant in H4/H5. In locations with high salinity levels (H6 to H8), the genera *Ilumatobacter*, *Nitriliruptor*, *Oceanicella*, *Entotheonella,* and *Aquipuribacter* were more abundant. These patterns suggest that microenvironmental differences across locations, such as moisture, salinity, nutrient content, or root exudate profiles, could be major drivers of bacterial community structure.

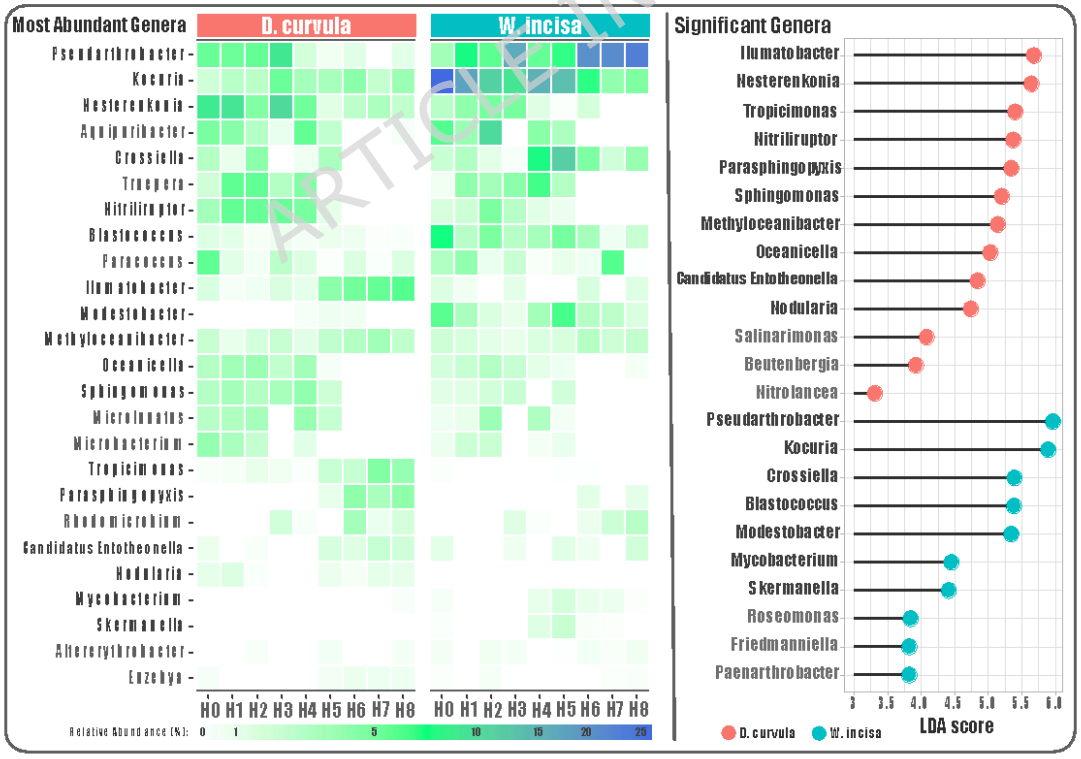

Figure 5. **Most abundant genera among the studied communities**. On the left: Heatmap showing the 25 most abundant bacterial lineages (ASVs) among all the studied sites for both plant species. The color gradient

indicates the relative abundance for each taxon. On the right: Linear discriminant analysis Effect Size of enriched genera for each plant species.

To further understand the structure and ecological roles of rhizosphere bacterial communities within *D. curvula* and *W. incisa*, we constructed co-occurrence networks based on significant correlations among ASVs. The networks reveal distinct topological patterns and taxonomic profiles between the two plant species (Figure 6, upper panel). In the *D. curvula* network, keystone ASVs had 45 nodes and 60 edges (39 positive and 21 negative interactions), with an average degree of 1.90, a global clustering coefficient of 0.152, and a modularity of 0.523. They included members of *Truepera* sp., *Rhodomicrobium* sp., *Oceanicella* sp., and *Sphingomonas* sp. (from the Deinococcota and Pseudomonadota phyla). The *W. incisa* network exhibited 33 nodes, 33 edges (21 positive and 12 negative interactions), an average degree of 1.05, a global clustering coefficient of 0.136, and a modularity of 0.638, and a more diverse set of keystone species, including *Pseudarthrobacter* sp., *Nesterenkonia* sp., *Blastococcus* sp., *Nitriliruptor* sp., and *Parasphingopyxis* sp. (mainly affiliated with Actinobacteriota, Deinococcota, and Pseudomonadota phyla). Some negative associations were also observed, potentially indicative of competitive exclusion or niche partitioning [69]. Network visualization was performed after removing isolated nodes; quantitative metrics were calculated on the full networks prior to node removal (62 and 63 nodes for *D. curvula* and *W. incisa* respectively) to avoid bias in metric estimation. In addition, we identified 12 taxa present in at least 80% of all samples analyzed for both plant species, which we considered the core microbiome (Figure 6, bottom panel). Moreover, six of these (order Rhizobiales, class KD4-96 (Chloroflexi), class Alphaproteobacteria, class GS-136 (Chloroflexi), order Actinomarinales, and family Euzebyaceae) were shared by all rhizospheric communities, indicating a core group of generalist microbes. While some other taxa were more prevalent in either *D. curvula* (family Nitriliruptoraceae and *Nesterenkonia* sp.) or *W. incisa* (*Kocuria* sp., family Geminicoccaceae, *Pseudarthrobacter* sp., and *Blastococcus* sp.), supporting the existence of host-specific microbial assemblages.

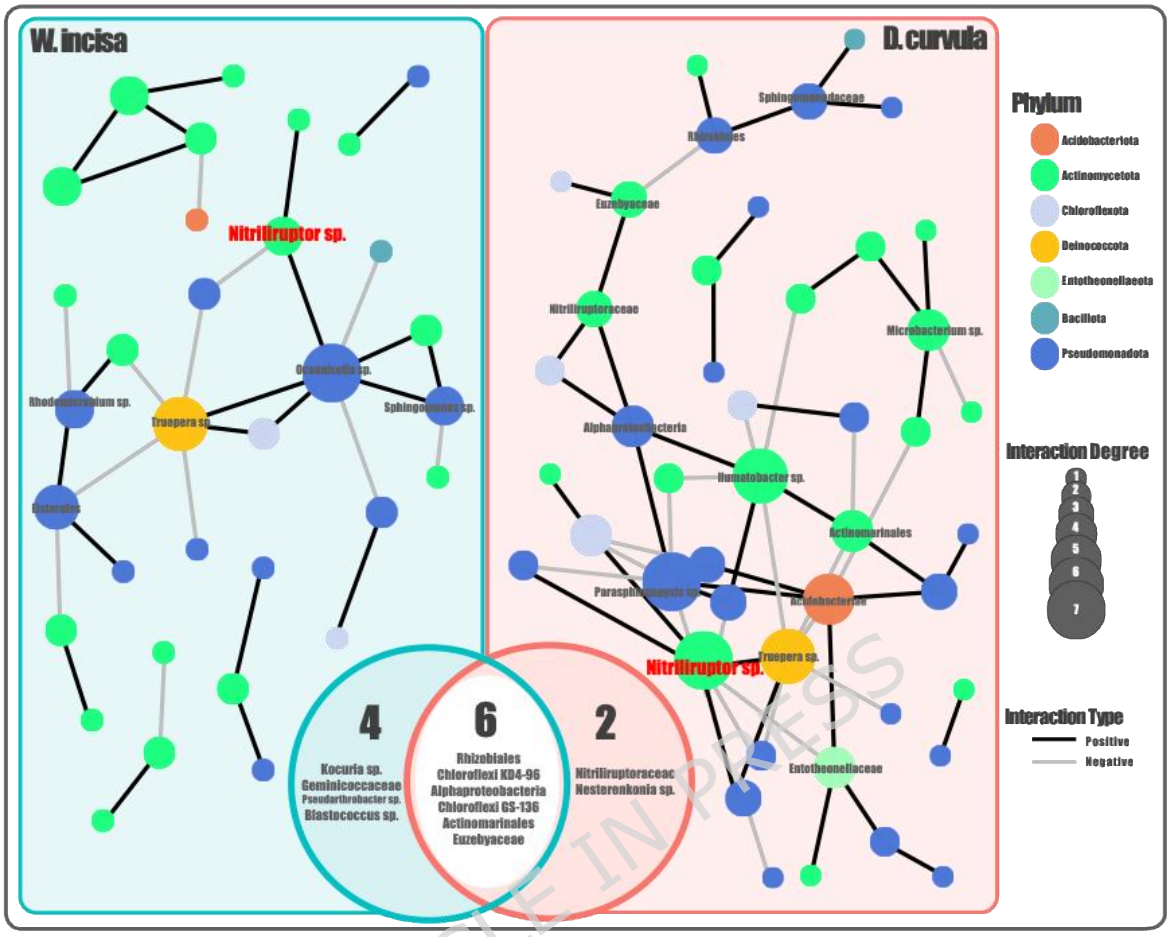

Figure 6. Co-occurrence networks and keystone species for the bacterial communities of both plant soils. The size of each node (representing ASVs) is proportional to the number of different interactions (degrees). The edges (significant connections between nodes) are colored to represent the interaction type. The node color indicates the taxonomic affiliation at the phylum level, and node labels indicate the identified keystone species. The Venn diagram illustrates the taxa detected in at least 80% of the soil samples for each plant, highlighting those that are exclusive to one plant and those that are common to both. All detected taxa were classified at the lowest available taxonomic rank.

We measured several physicochemical parameters to evaluate the influence of environmental variables on the rhizospheric communities of both plants. We found distinct site-specific values and diverse patterns between the two plants (Figure 7A). Humidity, EC, and OM were significantly different between the two plants, specifically in the southernmost sites of SH (H5 to H8), where the values increased significantly for *D. curvula*. Also, for this plant, we can observe some peaks, such as in total carbon and nitrogen for site

H6. The rhizospheric soils of *W. incisa* appear to be more stable across the variables evaluated, but pH was the only parameter that remained equivalent in the soils of both plants. The concentration of 10 chemical elements (As, Li, Zn, Fe, Cu, K, Ca, Mn, B, and Mg) in the rhizospheric soil samples was measured. Again, a clear differential pattern was observed across the locations and between plant species, reflecting what was described above for *D. curvula* (Figure 7B). Notably, elements such as Fe, K, and Mg exhibit relatively high concentrations in several sites, whereas toxic elements like As, Cu, and Zn display a more homogeneous distribution. Interestingly, at site H5, the elements As, Ca, B, Li, K, and Mg showed higher peaks for *D. curvula*-associated soils. There is a gradient of elemental composition that may influence microbial community dynamics and interactions with host plants.

The redundancy analysis shows a clear segregation between communities associated with each plant species (Figure 7C). We can also clearly observe a segregation between the samples from the northernmost areas of the SH (H0 to H4) and those from the southernmost sites (H5 to H8) for the communities associated with *D. curvula*. This separation is not observed in *W. incisa*. Several abiotic variables (Li, total Carbon, K, and B) were statistically significant and can help explain the observed clustering and segregation patterns, most of them driving the segregation of *D. curvula* communities. Moreover, humidity and Mg are drivers for the northernmost sites of the SH (H0 to H4), while total Nitrogen, EC, OM, Ca, and As are drivers for the southernmost sites (H5 to H8). Only Mn and Fe appear to explain clustering and segregation patterns in *W. incisa*.

By performing the redundancy analysis for each plant along the different locations, we were able to observe a much more evident segregation pattern for *D. curvula,* with the communities associated with plants from localities H0 to H4 forming a cluster and a second group with the communities associated with H6 to H8, leaving the communities of H5 separated (Figure 7D). This pattern is not as clear in the communities related to *W. incisa*, where a separation between samples H6 to H8 and the rest is observed to a lesser degree.

There are more significant variables that drive this segregation in *D. curvula*. Among the most notable findings, we observed that EC, As, and Ca strongly drive plants toward the southernmost area of SH (toward H8) at varying intensities. Still, OM, total carbon, and total nitrogen are significant only for *D. curvula*. Additionally, Humidity, pH, and elements such as Mg, Fe, Mn, Cu, and Zn are more closely associated with northern sites on SH. In contrast, others, such as Li, B, and K, exhibit a different pattern between the two plants. The clustering of sites to these variables reflects localized environmental conditions that distinctly affect the rhizospheric communities of each plant.

To further explore how environmental factors influence microbial community composition, we evaluated Spearman correlations between the most abundant genera and key abiotic variables in the rhizospheric soils of both plant species (Supplementary Figure S2). The analysis revealed distinct patterns of correlation between bacterial taxa and soil variables (pH, OM, humidity, and EC) across several sampling locations. In *D. curvula*, different genera were significantly influenced by environmental conditions. *Sphingomonas* exhibited a strong negative correlation with EC, whereas *Nesterenkonia* showed a negative correlation with humidity and a positive correlation with OM. *Ilumatobacter* exhibited location-dependent correlations with EC, OM, and pH. Likewise, *Nitriliruptor* displayed multiple correlations that varied by site with EC, pH, and humidity.

Additionally, genera such as *Oceanicella* and *Methyloceanibacter* exhibited significant correlations with all four abiotic variables. In contrast, for *W. incisa*, genera including *Paenarthrobacter*, *Pseudarthrobacter*, *Crossiella*, *Modestobacter*, and *Blastococcus* showed significant correlations with pH and EC, with variable correlations (positive or negative) across locations. These findings underscore the combined influence of local soil conditions and host plants on the rhizospheric communities.

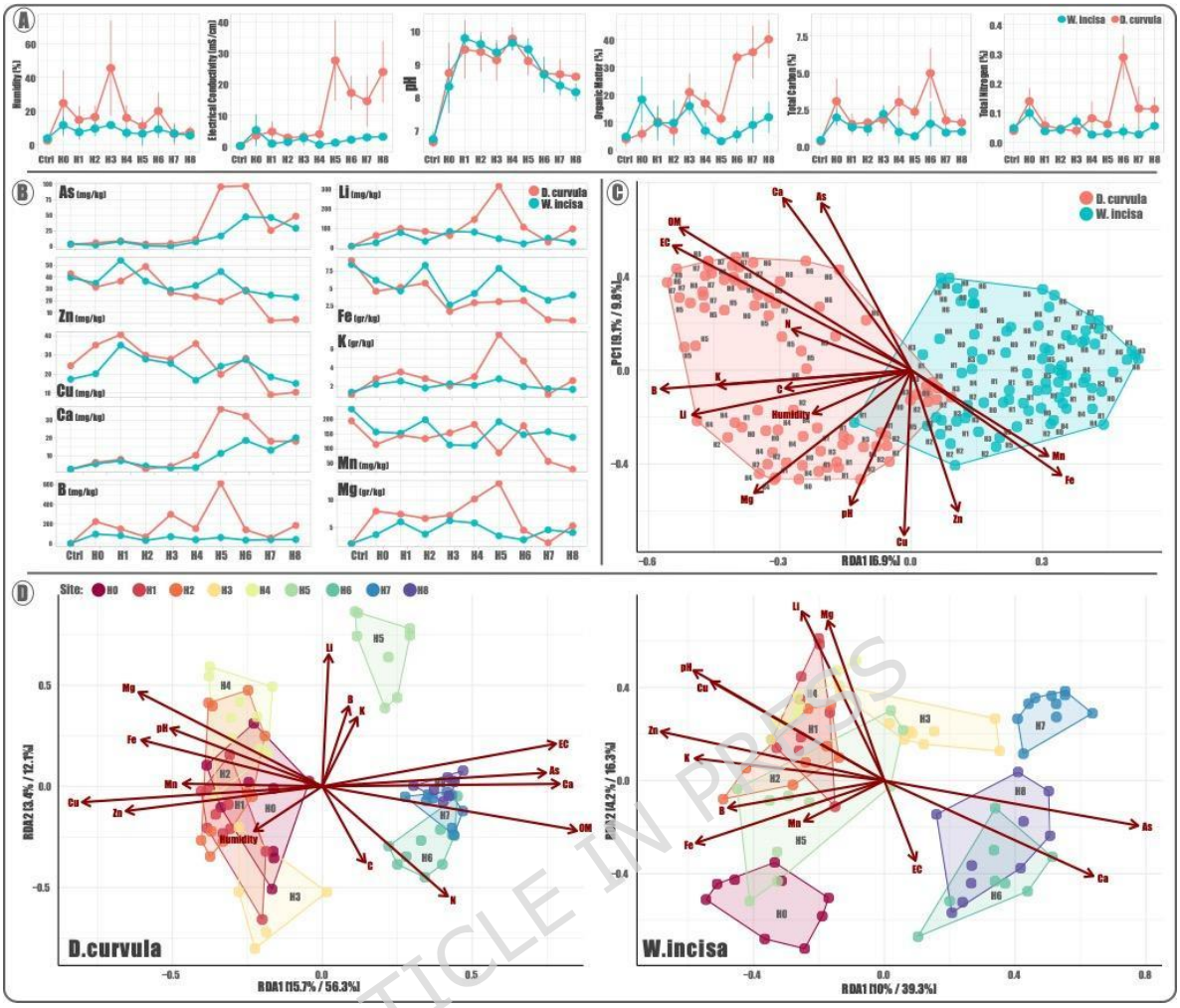

Figure 7. **Influence of Abiotic Factors on Community Structure and Composition**. Evaluation of A) Physicochemical parameters and B) Element concentrations in the rhizospheric soil samples throughout the studied sites for both plant species. Each point represents the average of a technical duplicate for every soil sample associated with the plant species at that site. Redundancy analysis of Hellinger-transformed community composition data comparing C) both plant species; D) the studied sites for *D. curvula* (left) and *W. incisa* (right). The arrows indicate the explanatory power of the statistically significant ($p < 0.05$) abiotic parameters in relation to the observed variation in community composition. The percentage of variance explained is depicted on the axis.

Estimation of the functional potential from both rhizobiomes revealed notable differences in the relative abundance of predicted ecologically relevant metabolic pathways across SH locations (Figure 8). Chemoheterotrophy and aerobic chemoheterotrophy were the dominant predicted metabolic strategies in both rhizobiomes, consistently representing

35–45% of the relative abundance across all sites, with particularly strong enrichment in *D. curvula* at sites H1, H3, and H6. In contrast, *W. incisa* rhizobiomes exhibited consistently higher relative abundances of bacteria putatively capable of denitrification, including predicted nitrate, nitrite, and nitrous oxide reduction, most notably at sites H2, H4, and H7. Fermentation was also detected as a distinct functional category, with a more consistent signal in *W. incisa* across multiple sites, suggesting the presence of anaerobic metabolic activity in this plants rhizosphere. Both plant-associated communities showed representation of predicted phototrophy-related functions; however, these could be distinguished into two functionally distinct strategies: oxygenic photoautotrophy and photosynthetic Cyanobacteriota, which were slightly more enriched in *D. curvula* at sites H0 and H8, and photoheterotrophy, which showed a differential distribution between the two plants along the SH. Furthermore, *W. incisa* rhizobiomes uniquely harbored putative functions associated with methylotrophy, methanol oxidation, and ureolysis, which are mostly absent or undetected in *D. curvula*. These results support the differential structuring of predicted microbial functional potential driven by host plant identity and localized environmental conditions.

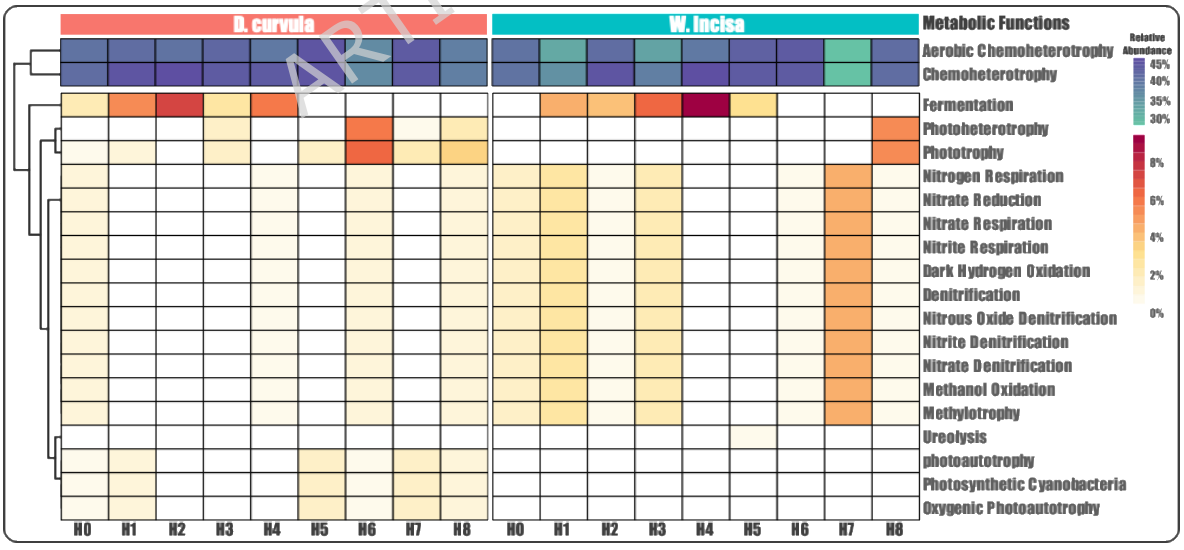

Figure 8. Predicted ecologically relevant pathway profiles for the communities of the rhizospheric soils of both plant species. The color scale represents the relative abundance of species known to carry the functional potential to perform the evaluated metabolic pathways.

Specific metabolic functions were further explored through taxonomy-based functional prediction to compare the profiles of *D. curvula* and *W. incisa* rhizospheric bacterial communities (Supplementary Figure S3). This analysis identified 30 metabolic pathways and biological functions that differed significantly between the two plant rhizobiomes (FDR-adjusted $p < 0.05$). Most of the putative enriched functions were associated with the rhizosphere of *W. incisa*, including predicted core metabolic pathways such as the pyruvate dehydrogenase complex, the tricarboxylic acid (TCA) cycle, S-adenosyl-L-methionine (SAM) cycle I and the glyoxylate bypass. In addition, degradation pathways for complex carbohydrates and aromatic compounds such as starch degradation, L-rhamnose degradation, and 3-phenylpropanoate degradation were more prevalent in *W. incisa* communities. Predicted functions related to teichoic acid biosynthesis and sulfur metabolism (e.g., sulfoglycolysis) were also enriched.

In contrast, fewer predicted functional categories were significantly enriched in *D. curvula* rhizobiomes; among them were pathways involved in the degradation of catechol and glycine betaine, and the biosynthesis of phylloquinol, peptidoglycan, and 1,4-dihydroxy-2-naphthoate. Notably, the most enriched functions were sulfolactate degradation in *D. curvula* and L-1,2-propanediol and starch degradation in *W. incisa*. Overall, these results suggest that *W. incisa* harbors a more putatively functionally diverse bacterial community, while *D. curvula* may carry a narrower but potentially more specialized rhizobiome.

DISCUSSION

The characterization of rhizospheric microbial communities associated with *D. curvula* and *W. incisa* across the Salar de Huasco reveals that both host plant identity and environmental gradients act as complementary and interactive forces shaping rhizobiome composition, structure, and functional potential in a polyextreme ecosystem. Rather than reflecting a single dominant driver, the patterns observed here emerge from the interplay between

plant-mediated selection (root exudate chemistry, nutrient demand, and physiological traits) and the strong abiotic pressures imposed by the SH salinity gradient, metal concentrations, and organic matter availability. The clear north-to-south pattern in plant distribution was mirrored by a similar divergence in their associated rhizobiomes, particularly for *D. curvula*, consistent with previous studies showing that plant biogeography and ecotypic variation significantly shape rhizosphere microbial diversity and assembly processes [70,71]. Critically, the two plant species appear to have converged on contrasting rhizobiome strategies: *D. curvula* supports a more diverse, spatially variable, and environmentally sensitive microbial community enriched in stress-tolerance and carbon-mineralization functions, while *W. incisa* harbors a comparatively stable, generalist rhizobiome with distinct nitrogen-cycling and anaerobic metabolic capabilities. These contrasting strategies likely reflect the different physiological demands and ecological niches of the two plants within SH and suggest that rhizobiome assembly in polyextreme environments is not random but rather represents an adaptive outcome of long-term plant-microbe coevolution under multiple simultaneous stressors.

Diversity analyses showed that *D. curvula* supported rhizospheric communities that were significantly richer than those of *W. incisa*. These differences were most pronounced in the southern SH sites, which had high salinity and metal concentrations. Similar changes in rhizobiome composition have been previously reported for plants like *Robinia pseudoacacia* across large spatial scales [72]. Additionally, the lack of notable differences between rhizosphere and rhizoplane compartments aligns with findings in desert-adapted plants, where the physical and chemical gradients that normally differentiate root-associated microhabitats may be compressed or homogenized by the predominant influence of extreme abiotic conditions, resulting in overlapping microbial communities across root-associated zones [73].

Taxonomic profiling showed Actinomycetota as the main phylum across both plant species, with genera such as *Pseudarthrobacter*, *Modestobacter*, and *Blastococcus* contributing to

species-specific community profiles. The dominance of Actinomycetota in both rhizobiomes reflects the remarkable evolutionary adaptations that make this phylum uniquely suited to polyextreme environments. Actinobacteria thriving in high-altitude Andean ecosystems harbor a "UV-resistome" encompassing UV sensing, DNA damage repair, and oxidative stress response mechanisms that enable survival under extreme irradiation [74]. At the genus level, *Modestobacter* exhibits high tolerance to UV irradiation, desiccation, and oxidative stress, linked to its radiation resistance profile and photoprotective pigment synthesis [75], while *Blastococcus* possesses a large accessory genome conferring genomic plasticity that underpins its capacity for substrate degradation and tolerance to drought, salinity, and heavy metal contamination [81]. The enrichment of families like Micrococcaceae in *W. incisa* and Euzebyaceae in *D. curvula* may also indicate host-specific microbial selection, as seen in different plant cultivars [23,76].

The differential enrichment of specific genera identified by LEfSe, including *Nesterenkonia*, *Nitrolancea*, and *Ilumatobacter* in *D. curvula* and *Paenarthrobacter*, *Friedmanniella*, and *Roseomonas* in *W. incisa* further supports the existence of host-specific microbial selection patterns, suggesting that each plant species actively shapes its rhizosphere bacterial community through selective recruitment, likely mediated by differences in root exudate composition and physicochemical microenvironments.

Actinomycetota genera *Pseudarthrobacter* and *Modestobacter* have been linked to resilience under harsh environmental conditions [77,78], and these were enriched in *D. curvula*-associated rhizobiomes. Others, such as *Blastococcus*, *Mycobacterium*, and *Kocuria,* were often detected at relatively high levels, indicating they may be common members of rhizosphere communities in these arid environments, as previously reported in desert areas and metal-contaminated soils.

Interestingly, some genera showed strong habitat- or host-specific enrichment. In *W. incisa*-associated rhizobiomes, the genus *Skermanella* was abundant, which has been associated

with plants under arid or semi-arid conditions, showing adaptation to stress or nutrient limitations [82]. Also, the Cyanobacteriota *Nodularia* are characterized as nitrogen-fixers that can thrive in high-salinity, nutrient-poor, and UV-exposed environments [83]. On the other hand, *Crossiella*, *Microbacterium*, Candidatus Entotheonella, *Ilumatobacter,* and *Microlunatus* were more abundant in *D. curvula* rhizobiomes. All these genera have been associated with promoting plant growth and producing secondary metabolites under arid conditions [84–88], highlighting the functional potential of these communities.

D. curvula hosts a rhizobiome dominated by Actinomycetota adapted to arid and nutrient-poor soils, with several enriched taxa known for plant-growth-promoting traits. Meanwhile, *W. incisa* harbors more halotolerant and nitrogen-metabolizing taxa, indicating adaptation to saline or harsh soil conditions and potentially a different approach to plant–microbe interactions. The progressive shift in dominant Actinomycetota genera across SH localities (from *Mycobacterium* and *Modestobacter* in the northern sites to *Microlunatus* and *Truepera* in the transitional zones and *Ilumatobacter* and *Entotheonella* in the southern high-salinity sites) is consistent with a community succession driven by the intensification of abiotic stress along the north-to-south gradient. This pattern suggests that as salinity, metal concentrations, and osmotic stress increase southward, the rhizobiome undergoes a directional filtering toward taxa with increasingly specialized stress-tolerance traits, reflecting the sequential replacement of generalist Actinomycetota with more halotolerant and metal-resistant lineages.

Network analysis showed greater complexity and interaction density in *D. curvula*, as reflected by its higher number of edges (59 vs. 33) and nearly double the average degree (1.90 vs. 1.05) compared to *W. incisa*, with several high-degree keystone ASVs linked to stress-adapted genera like *Truepera* and *Sphingomonas* [89,90]. From an ecological theory perspective, this higher connectivity is consistent with greater functional redundancy, providing the community with higher resilience against the loss of individual members under stress. The central position of *Truepera* in the *D. curvula* network is particularly

relevant in this context, as this genus is renowned for its exceptional resistance to ionizing radiation, robust DNA repair mechanisms, and tolerance to alkaline and saline conditions [91], suggesting it may act as a structural anchor maintaining community stability under the fluctuating abiotic conditions of SH. Similarly, *Sphingomonas* species have been shown to improve plant growth under drought, salinity, and heavy metal stress conditions, and their gene content has been shown to reflect habitat preference, stress tolerance and resource acquisition [92] which is consistent with its role as a keystone taxon in the *D. curvula* network.

The predominance of positive interactions in both networks suggests that cooperative or syntrophic relationships are a general feature of rhizosphere microbial communities in this ecosystem, potentially reflecting the mutualistic dependencies that arise under the nutrient-limited and polyextreme conditions characteristic of SH. In environments with resources scarcity, positive microbial interactions are thought to be favored over competitive interactions, as cooperation may provide a collective advantage for survival under multiple simultaneous stressors. Nevertheless, the higher proportion of positive edges and overall network complexity observed in *D. curvula* suggest that this plant rhizobiome may sustain a more elaborated cooperative structure, which could underpin greater ecological resilience and functional redundancy when facing environmental stress. It has been previously stated that microbial communities with more complex network structures are more resilient to abiotic stress in degraded grasslands [71,93]. The negative interactions observed in both networks, while less frequent, may reflect competitive exclusion or niche partitioning among community members, processes that are not mutually exclusive with the broader cooperative dynamic of the community. In contrast, the simpler network in *W. incisa* indicates a less interconnected microbial structure, which could make it more vulnerable to disturbance despite the cooperative nature of its interactions.

Integrating the taxonomic, network, and functional evidence, the rhizobiomes of *D. curvula* and *W. incisa* emerge as representatives of two contrasting ecological strategies for survival in a polyextreme environment. *D. curvula* follows a specialization and resilience strategy: higher diversity, greater network complexity, dominance of stress-adapted Actinomycetota with UV resistance and desiccation tolerance, and enrichment of functions related to osmotic tolerance, photoprotection, and compounds degradation, suggesting a rhizobiome well adapted to provide broad-spectrum stress protection. In contrast, *W. incisa* follows a nutritional versatility strategy: a stable, generalist community less sensitive to local edaphic conditions, enriched in diverse carbon and nitrogen cycling pathways (denitrification, fermentation, methylotrophy, ureolysis, and central metabolic routes) suggesting a microbiome that maximizes nutrient acquisition flexibility as an alternative means of coping with environmental unpredictability. These contrasting strategies likely reflect the different ecological niches of the two plant species within SH and highlight the diversity of plant-microbe interactions that can emerge within a single extreme ecosystem.

Environmental variables played a central role in driving microbial composition, particularly for *D. curvula*, where EC and OM were significantly associated with microbial shifts; the same was observed for elements such as Li and As, which were detected in high concentrations (317.1 mg/kg and 97.1 mg/kg, respectively). These findings are consistent with soil microbiome studies in extreme environments, which show that physicochemical properties and heavy metal concentrations are significant determinants of microbial community structure [94–96]. The contrasting patterns observed between the two plants are particularly informative in this regard: while *D. curvula* communities were strongly structured by a broad set of abiotic variables (Li, total carbon, K, B, humidity, Mg, total nitrogen, EC, OM, Ca, and As) with clear differentiation between northern and southern sites; *W. incisa* communities were primarily associated with only Mn and Fe, and showed comparatively little spatial structuring across the SH gradient. This asymmetry suggests that *D. curvula* rhizobiomes are more sensitive to, or more strongly selected by local soil chemistry, while *W. incisa* may harbor a more generalist microbial community less

dependent on specific edaphic conditions. Taken together, these results indicate that rhizobiome composition in the SH is shaped by the combined and interactive influence of soil chemistry and host plant identity (neither factor alone being sufficient to explain the observed community patterns) consistent with the growing consensus that plant-soil feedbacks are key drivers of rhizosphere microbial assembly across environmental gradients [97].

Broad level functional predictions revealed clear metabolic differentiation between the rhizobiomes of *D. curvula* and *W. incisa*, suggesting distinct putative nutrient acquisition strategies and stress-response mechanisms. The dominance of predicted chemoheterotrophy across both rhizobiomes reflects the heterotrophic nature of soil microbial communities fueled by root exudates and organic matter inputs, as root exudates provide soil microbes with important precursors that regulate carbon input and microbial activity in the rhizosphere [98] and is consistent with the carbon-limited conditions typical of high-altitude arid soils. The stronger enrichment of these predicted functions in *D. curvula* at sites H1, H3, and H6 may be linked to the higher organic matter values recorded at those sites, suggesting a tighter coupling between plant-derived carbon inputs and microbial carbon mineralization activity, a pattern consistent with the microbial mining hypothesis, whereby microbes use root exudate-derived energy to release nutrients locked in soil organic matter [99]. The consistently higher abundance of taxa capable of denitrifying in *W. incisa* rhizobiomes is ecologically significant, as this is the most energetically favorable respiratory pathway in the absence of oxygen, and salinity has been shown to directly affect the distribution patterns and community composition of denitrifiers [100], suggesting that the higher salinity characteristic of several *W. incisa* sampling sites may be driving the enrichment of nitrate-respiring bacteria as an alternative respiratory strategy. This has direct implications for nitrogen availability to the host plant, as nitrogen lost through denitrification to N_2 reduces the pool of plant-available nitrogen in the rhizosphere.

The variation in predicted phototrophic functions along the north-to-south gradient of SH detected on *D. curvula* rhizobiomes may reflect the sensitivity of these putative functional groups to salinity, as high salt concentrations can damage the photosynthetic apparatus, inhibit the synthesis of photosystem-related proteins, and destroy thylakoid membrane structure, leading to inhibited photosynthesis in cyanobacteria [101], which would be consistent with the reduced photosynthetic signal observed in the high-salinity southern sites. Moreover, predicted fermentation was enriched in *W. incisa* rhizobiomes, further supports the presence of anaerobic microbial activity in this plant's rhizosphere, consistent with evidence that the ability to perform alternative respiratory strategies such as denitrification and fermentation provides a competitive advantage in microbiomes exposed to fluctuating oxygen availability [102]. Finally, the exclusive enrichment of methylotrophy and ureolysis in *W. incisa* rhizobiomes is interesting, as these bacteria promote plant growth through nitrogen fixation, phosphate solubilization, phytohormone production, and ACC deaminase activity, which have been shown to exhibit superior stress-tolerating capacity against drought, salinity, and UV radiation [103]. Simultaneously, putative ureolytic bacterial communities contribute to nitrogen mineralization rates in the rhizosphere, with urease activity playing a key role in converting organic nitrogen to plant-available ammonium [104]. The co-occurrence of these predicted functions exclusively in *W. incisa* suggests that this plant selectively recruits microbial groups capable of expanding nitrogen and carbon acquisition strategies, potentially compensating for the lower predicted chemoheterotrophic activity observed in its rhizobiome compared to *D. curvula*.

Beyond taxonomic patterns, the predicted functional profiles of both rhizobiomes at a more specific level offer ecologically and agriculturally relevant insights. Among the pathways predicted to be significantly enriched in *D. curvula* rhizobiomes (Supplementary Figure S3), glycine betaine degradation stands out as particularly noteworthy. Glycine betaine is one of the most commonly produced osmoprotectants by bacteria and has been shown to significantly enhance the salinity tolerance of rhizobacteria [105], and its predicted active cycling in the *D. curvula* rhizosphere suggests that associated bacteria may putatively

contribute to osmotic stress buffering which is a relevant trait to plant performance under saline and drought conditions. Additionally, the predicted enrichment of phylloquinone biosynthesis pathways points to putative microbial support of photosynthetic function, given that phylloquinone (vitamin K1) serves as an essential electron carrier in Photosystem I in photosynthetic organisms, with particular relevance under the intense UV radiation characteristic of the Altiplano [106]. Predicted catechol degradation pathways were also enriched in *D. curvula*, indicating a putative capacity to detoxify aromatic compounds and potentially mitigate the effects of the metal-contaminated soils which is also characteristic of this ecosystem. In contrast, *W. incisa* rhizobiomes showed significant enrichment of the S-adenosyl-L-methionine (SAM) cycle, which can be converted to ACC by the enzyme ACC synthase, thereby putatively diminishing the synthesis of plant growth-inhibitory ethylene [37]. The predicted enrichment of this pathway suggests that *W. incisa* may participate in hormone-mediated plant–microbe interactions that mitigate ethylene accumulation induced by stress, a key regulator mechanism for plants growing under harsh environmental conditions [107]. Furthermore, the predicted enrichment of sulfoglycolysis in *W. incisa* communities suggests putative active cycling of sulfolipids within the rhizosphere. This process likely contributes to the microbial mobilization of organosulfur compounds, which is essential for converting soil sulfur into plant-bioavailable sulfate [108]. In this context, sulfur-cycling microorganisms in the rhizosphere have been shown to promote plant growth and crop yield through multiple mechanisms, including enhanced nutrient mobilization and mitigation of abiotic stress [109].

Taken together, these predicted functional differences suggest that the two rhizobiomes use distinct but complementary strategies for supporting plant survival under polyextreme conditions, with the *D. curvula* rhizobiome appearing particularly enriched in predicted functions associated with osmotic and oxidative stress tolerance. These findings reinforce the central argument that rhizobiome assembly in the SH reflects an adaptive outcome of plant-microbe coevolution under multiple simultaneous stressors and highlight the potential of these extreme-environment microbiomes as reservoirs of functionally relevant

taxa for future biotechnological applications aimed at improving crop resilience under arid and saline conditions.

CONCLUSION

This study demonstrates that the rhizospheric microbial communities of *D. curvula* and *W. incisa* in the Salar de Huasco are shaped by the combined influence of host plant identity and local environmental gradients, giving rise to two ecologically distinct rhizobiomes representing contrasting survival strategies in a polyextreme ecosystem: a specialization and resilience strategy in *D. curvula*, and a nutritional versatility strategy in *W. incisa*. Beyond their scientific interest, these findings carry implications that extend well beyond microbial ecology. The microbial communities characterized here comprise a largely unexplored and highly diverse assemblage (both taxonomically and functionally), that remains mostly overlooked in current conservation frameworks. The Salar de Huasco is a protected Ramsar wetland, yet like most protected areas in Chile, its conservation status does not consider microbial diversity, which is a critical gap given that these communities have been shaped by millions of years of coevolution and their loss would be irreversible. From a biotechnological perspective, the stress-tolerance functions identified here (osmoprotection, UV resistance, DNA repair, and specialized nutrient cycling) represent an underexplored genetic reservoir for developing microbial inoculants aimed at improving crop resilience under arid and saline conditions. Realizing this potential, however, requires that these communities are first conserved in situ, underscoring the fundamental link between biodiversity conservation and biotechnological innovation.

AUTHOR CONTRIBUTIONS

JC-S and FR conceived and designed the study. JC-S, JF, ECN, and FR performed the field work. JC-S processed the samples and performed the experimental procedures. JC-S carried out the bioinformatics analyses. JS and UNdR performed DNA library construction and

amplicon sequencing. CPS, ECN, RM, RB, VHA, UNdR and FR contributed with advice, reagents, materials, and analysis tools. JC-S and CP-E interpreted the results and wrote the first manuscript draft. All authors read and approved the final manuscript.

FUNDING

This research was sponsored by ANID (Agencia Nacional de Investigación y Desarrollo de Chile) grants. JCS and FR ANID 2021 Postdoctoral FONDECYT 3210156, ANID Regular FONDECYT 1220902 and ANID Anillo ATE240012; CPE ANID 2021 Postdoctoral FONDECYT 3230189. CS ANID Regular FONDECYT 1250419 and ANID Anillo ATE220007; ECN ANID FONDECYT 1240871. The funders had no role in study design, data collection and analysis, decision to publish, or preparation of the manuscript.

CONFLICT OF INTEREST STATEMENT

The authors declare that the research was conducted in the absence of any commercial or financial relationships that could be construed as a potential conflict of interest.

REFERENCES

1. Niu B, Paulson JN, Zheng X, Kolter R. Simplified and representative bacterial community of maize roots. Proceedings of the National Academy of Sciences. National Academy of Sciences; 2017;114:E2450–9.

2. Pereira LS. Water, agriculture and food: challenges and issues. Water Resources Management. Springer; 2017;31:2985–99.

3. Scoones I, Smalley R, Hall R, Tsikata D. Narratives of scarcity: Framing the global land rush. Geoforum. Elsevier; 2019;101:231–41.

4. Placzek C, Quade J, Patchett PJ. Geochronology and stratigraphy of late Pleistocene lake cycles on the southern Bolivian Altiplano: implications for causes of tropical climate change. Geological Society of America Bulletin. Geological Society of America; 2006;118:515–32.

5. Orellana R, Macaya C, Bravo G, Dorochesi F, Cumsille A, Valencia R, et al. Living at the frontiers of life: extremophiles in Chile and their potential for bioremediation. Frontiers in Microbiology. Frontiers Media SA; 2018;9:2309.

6. Azua-Bustos A, González-Silva C, Corsini G. The Hyperarid Core of the Atacama Desert, an Extremely Dry and Carbon Deprived Habitat of Potential Interest for the Field of Carbon Science. Front Microbiol [Internet]. Frontiers; 2017 [cited 2025 Nov 13];8. https://doi.org/10.3389/fmicb.2017.00993

7. Cabrol NA, Grin EA, Zippi P, Noffke N, Winter D. Evolution of altiplanic lakes at the pleistocene/holocene transition: a window into early mars declining habitability, changing habitats, and biosignatures. From Habitability to Life on Mars. Elsevier; 2018. p. 153–77.

8. Vivanco L, Rascovan N, Austin AT. Plant, fungal, bacterial, and nitrogen interactions in the litter layer of a native Patagonian forest. PeerJ. PeerJ Inc.; 2018;6:e4754.

9. Bal HB, Das S, Dangar TK, Adhya TK. ACC deaminase and IAA producing growth promoting bacteria from the rhizosphere soil of tropical rice plants. Journal of basic microbiology. Wiley Online Library; 2013;53:972–84.

10. Hernández KL, Yannicelli B, Olsen LM, Dorador C, Menschel EJ, Molina V, et al. Microbial activity response to solar radiation across contrasting environmental conditions in Salar de Huasco, Northern Chilean Altiplano. Frontiers in Microbiology. Frontiers Media SA; 2016;7:1857.

11. Castro-Severyn J, Pardo-Esté C, Sulbaran Y, Cabezas C, Gariazzo V, Briones A, et al. Arsenic response of three altiplanic Exiguobacterium strains with different tolerance levels against the metalloid species: a proteomics study. Frontiers in Microbiology. Frontiers Media SA; 2019;10:2161.

12. Cortés-Albayay C, Silber J, Imhoff JF, Asenjo JA, Andrews B, Nouioui I, et al. The polyextreme ecosystem, Salar de Huasco at the Chilean Altiplano of the Atacama Desert houses diverse Streptomyces spp. with promising pharmaceutical potentials. Diversity. MDPI; 2019;11:69.

13. Castro-Severyn J, Pardo-Esté C, Mendez KN, Morales N, Marquez SL, Molina F, et al. Genomic variation and arsenic tolerance emerged as niche specific adaptations by different

Exiguobacterium strains isolated from the extreme Salar de Huasco environment in Chilean–Altiplano. Frontiers in Microbiology. Frontiers Media SA; 2020;11:1632.

14. Dorador C, Molina V, Hengst M, Eissler Y, Cornejo M, Fernández C, et al. Microbial Communities composition, activity, and dynamics at salar de huasco: a polyextreme environment in the chilean altiplano. Microbial ecosystems in central andes extreme environments: biofilms, microbial mats, microbialites and endoevaporites. Springer; 2020. p. 123–39.

15. Pérez V, Hengst M, Kurte L, Dorador C, Jeffrey WH, Wattiez R, et al. Bacterial survival under extreme UV radiation: a comparative proteomics study of Rhodobacter sp., isolated from high altitude wetlands in Chile. Frontiers in microbiology. Frontiers Media SA; 2017;8:1173.

16. Schell CM, Waterway MJ. Allozyme variation and the genetic structure of populations of the rare sedge Carex misera (Cyperaceae). Plant Species Biology. Wiley Online Library; 1992;7:141–50.

17. de Ugaz OL. Avances en el estudio del género Werneria y sus metabolitos secundarios. Revista de química. 1998;12:69–85.

18. Rodríguez MF, Rúgolo de Agrasar ZE, Aschero C. El género Deyeuxia (Poaceae, Agrostideae) en sitios arqueológicos de la Puna meridional argentina, provincia de Catamarca. Chungará (Arica). SciELO Chile; 2003;35:51–72.

19. Castellaro G, Ullrich T, Wackwitz B, Raggi A. Composición botánica de la dieta de alpacas (Lama pacos L.) y llamas (Lama glama L.) en dos estaciones del año, en praderas altiplánicas de un sector de la Provincia de Parinacota, Chile. Agricultura técnica. SciELO Chile; 2004;64:353–63.

20. Rámila CD, Leiva ED, Bonilla CA, Pastén PA, Pizarro GE. Boron accumulation in Puccinellia frigida, an extremely tolerant and promising species for boron phytoremediation. Journal of Geochemical Exploration. Elsevier; 2015;150:25–34.

21. Bonfante P, Anca I-A. Plants, mycorrhizal fungi, and bacteria: a network of interactions. Annual review of microbiology. Annual Reviews; 2009;63:363–83.

22. Vukanti RV. Structure and function of rhizobiome. Plant Microbe Symbiosis. Springer; 2020. p. 241–61.

23. Compant S, Samad A, Faist H, Sessitsch A. A review on the plant microbiome: ecology, functions, and emerging trends in microbial application. Journal of advanced research. Elsevier; 2019;19:29–37.

24. Richardson AE, Barea J-M, McNeill AM, Prigent-Combaret C. Acquisition of phosphorus and nitrogen in the rhizosphere and plant growth promotion by microorganisms. Springer; 2009.

25. Fuentes A, Herrera H, Charles TC, Arriagada C. Fungal and bacterial microbiome associated with the rhizosphere of native plants from the Atacama desert. Microorganisms. MDPI; 2020;8:209.

26. Trivedi P, Leach JE, Tringe SG, Sa T, Singh BK. Plant–microbiome interactions: from community assembly to plant health. Nature reviews microbiology. Nature Publishing Group UK London; 2020;18:607–21.

27. Hassani MA, Durán P, Hacquard S. Microbial interactions within the plant holobiont. Microbiome. Springer; 2018;6:58.

28. Puente ME, Li CY, Bashan Y. Endophytic bacteria in cacti seeds can improve the development of cactus seedlings. Environmental and Experimental Botany. Elsevier; 2009;66:402–8.

29. Giauque H, Hawkes CV. Climate affects symbiotic fungal endophyte diversity and performance. American journal of botany. Wiley Online Library; 2013;100:1435–44.

30. Torres-Diaz C, Gallardo-Cerda J, Lavin P, Oses R, Carrasco-Urra F, Atala C, et al. Biological interactions and simulated climate change modulates the ecophysiological performance of Colobanthus quitensis in the Antarctic ecosystem. PLoS One. Public Library of Science San Francisco, CA USA; 2016;11:e0164844.

31. Waller F, Achatz B, Baltruschat H, Fodor J, Becker K, Fischer M, et al. The endophytic fungus Piriformospora indica reprograms barley to salt-stress tolerance, disease resistance, and higher yield. Proceedings of the National Academy of Sciences. National Academy of Sciences; 2005;102:13386–91.

32. Redman RS, Kim YO, Woodward CJ, Greer C, Espino L, Doty SL, et al. Increased fitness of rice plants to abiotic stress via habitat adapted symbiosis: a strategy for mitigating impacts of climate change. PLOS one. Public Library of Science San Francisco, USA; 2011;6:e14823.

33. Molina-Montenegro MA, Oses R, Torres-Díaz C, Atala C, Zurita-Silva A, Ruiz-Lara S. Root-endophytes improve the ecophysiological performance and production of an agricultural species under drought condition. AoB Plants. Annals of Botany Company; 2016;8:plw062.

34. Santander C, Ruiz A, García S, Aroca R, Cumming J, Cornejo P. Efficiency of two arbuscular mycorrhizal fungal inocula to improve saline stress tolerance in lettuce plants by changes of antioxidant defense mechanisms. Journal of the Science of Food and Agriculture. Wiley Online Library; 2020;100:1577–87.

35. Egamberdieva D, Wirth SJ, Alqarawi AA, Abd_Allah EF, Hashem A. Phytohormones and beneficial microbes: essential components for plants to balance stress and fitness. Frontiers in microbiology. Frontiers Media SA; 2017;8:2104.

36. Patel VK, Srivastava R, Sharma A, Srivastava AK, Singh S, Srivastava AK, et al. Halotolerant Exiguobacterium profundum PHM11 tolerate salinity by accumulating L-proline and fine-tuning gene expression profiles of related metabolic pathways. Frontiers in microbiology. Frontiers Media SA; 2018;9:423.

37. Glick BR, Todorovic B, Czarny J, Cheng Z, Duan J, McConkey B. Promotion of plant growth by bacterial ACC deaminase. Critical reviews in plant sciences. Taylor & Francis; 2007;26:227–42.

38. López-Lozano NE, Echeverría Molinar A, Ortiz Durán EA, Hernández Rosales M, Souza V. Bacterial diversity and interaction networks of Agave lechuguilla rhizosphere differ significantly from bulk soil in the oligotrophic basin of Cuatro Cienegas. Frontiers in Plant Science. Frontiers Media SA; 2020;11:1028.

39. Prittesh P, Avnika P, Kinjal P, Jinal HN, Sakthivel K, Amaresan N. Amelioration effect of salt-tolerant plant growth-promoting bacteria on growth and physiological properties of rice (Oryza sativa) under salt-stressed conditions. Archives of Microbiology. Springer; 2020;202:2419–28.

40. Astorga-Eló M, Zhang Q, Larama G, Stoll A, Sadowsky MJ, Jorquera MA. Composition, predicted functions and co-occurrence networks of rhizobacterial communities impacting flowering desert events in the Atacama Desert, Chile. Frontiers in microbiology. Frontiers Media SA; 2020;11:571.

41. Taketani RG, Kavamura VN, Mendes R, Melo IS. Functional congruence of rhizosphere microbial communities associated to leguminous tree from B razilian semiarid region. Environmental microbiology reports. Wiley Online Library; 2015;7:95–101.

42. Demergasso C, Dorador C, Meneses D, Blamey J, Cabrol N, Escudero L, et al. Prokaryotic diversity pattern in high-altitude ecosystems of the Chilean Altiplano. Journal of Geophysical Research: Biogeosciences. Wiley Online Library; 2010;115.

43. Strahsburger E, Zapata F, Pedroso I, Fuentes D, Tapia P, Ponce R, et al. Draft genome sequence of Exiguobacterium aurantiacum strain PN47 isolate from saline ponds, known as “Salar del Huasco”, located in the Altiplano in the North of Chile. brazilian journal of microbiology. SciELO Brasil; 2018;49:7–9.

44. Remonsellez F, Castro-Severyn J, Pardo-Esté C, Aguilar P, Fortt J, Salinas C, et al. Characterization and salt response in recurrent halotolerant Exiguobacterium sp. SH31 isolated from sediments of Salar de Huasco, Chilean Altiplano. Frontiers in microbiology. Frontiers Media SA; 2018;9:2228.

45. Fortt J, González M, Morales P, Araya N, Remonsellez F, Coba de la Peña T, et al. Bacterial modulation of the plant ethylene signaling pathway improves tolerance to salt stress in lettuce (Lactuca sativa L.). Frontiers in Sustainable Food Systems. Frontiers Media SA; 2022;6:768250.

46. Knief C. Analysis of plant microbe interactions in the era of next generation sequencing technologies. Frontiers in plant science. Frontiers Media SA; 2014;5:216.

47. van der Heijden MG, Schlaeppi K. Root surface as a frontier for plant microbiome research. Proceedings of the National Academy of Sciences. National Academy of Sciences; 2015;112:2299–300.

48. Guajardo-Leiva S, Alarcón J, Gutzwiller F, Gallardo-Cerda J, Acuña-Rodríguez IS, Molina-Montenegro M, et al. Source and acquisition of rhizosphere microbes in Antarctic vascular plants. Frontiers in microbiology. Frontiers Media SA; 2022;13:916210.

49. Klindworth A, Pruesse E, Schweer T, Peplies J, Quast C, Horn M, et al. Evaluation of general 16S ribosomal RNA gene PCR primers for classical and next-generation sequencing-based diversity studies. Nucleic acids research. Oxford University Press; 2013;41:e1–e1.

50. Callahan BJ, McMurdie PJ, Rosen MJ, Han AW, Johnson AJA, Holmes SP. DADA2: High-resolution sample inference from Illumina amplicon data. Nature methods. Nature Publishing Group US New York; 2016;13:581–3.

51. Quast C, Pruesse E, Yilmaz P, Gerken J, Schweer T, Yarza P, et al. The SILVA ribosomal RNA gene database project: improved data processing and web-based tools. Nucleic acids research. Oxford University Press; 2012;41:D590–6.

52. Wang Q, Garrity GM, Tiedje JM, Cole JR. Naive Bayesian classifier for rapid assignment of rRNA sequences into the new bacterial taxonomy. Applied and environmental microbiology. American Society for Microbiology; 2007;73:5261–7.

53. Wright ES. Fast and Flexible Search for Homologous Biological Sequences with DECIPHER v3. R Journal. 2024;16.

54. Price MN, Dehal PS, Arkin AP. FastTree: computing large minimum evolution trees with profiles instead of a distance matrix. Molecular biology and evolution. Oxford University Press; 2009;26:1641–50.

55. McMurdie PJ, Holmes S. phyloseq: an R package for reproducible interactive analysis and graphics of microbiome census data. PloS one. Public Library of Science San Francisco, USA; 2013;8:e61217.

56. Love MI, Huber W, Anders S. Moderated estimation of fold change and dispersion for RNA-seq data with DESeq2. Genome biology. Springer; 2014;15:550.

57. Andersen KS, Kirkegaard RH, Karst SM, Albertsen M. ampvis2: an R package to analyse and visualise 16S rRNA amplicon data [Internet]. bioRxiv; 2018 [cited 2025 Nov 13]. p. 299537. https://doi.org/10.1101/299537

58. Xu S, Zhan L, Tang W, Wang Q, Dai Z, Zhou L, et al. MicrobiotaProcess: A comprehensive R package for deep mining microbiome. The Innovation. Elsevier; 2023;4.

59. Segata N, Izard J, Waldron L, Gevers D, Miropolsky L, Garrett WS, et al. Metagenomic biomarker discovery and explanation. Genome biology. Springer; 2011;12:R60.

60. Shetty SA, Lahti L, de Vos WM, Smidt H. microbiomeutilities: An R package for utilities to guide in-depth marker gene amplicon data analysis. Ecophysiological insights into the human intestinal microbiota: from single strains to defined consortia. 2018;95.

61. Kurtz ZD, Müller CL, Miraldi ER, Littman DR, Blaser MJ, Bonneau RA. Sparse and compositionally robust inference of microbial ecological networks. PLoS computational biology. Public Library of Science San Francisco, CA USA; 2015;11:e1004226.

62. Schloerke B, Cook D, Larmarange J, Briatte F, Marbach M, Thoen E, et al. GGally: Extension to'ggplot2'. 2021;

63. Ssekagiri AT, Sloan W, Ijaz UZ. microbiomeSeq: an R package for analysis of microbial communities in an environmental context. ISCB africa ASBCB conference. ISCB Kumasi; 2017.

64. Douglas GM, Maffei VJ, Zaneveld JR, Yurgel SN, Brown JR, Taylor CM, et al. PICRUSt2 for prediction of metagenome functions. Nature biotechnology. Nature Publishing Group US New York; 2020;38:685–8.

65. Kanehisa M, Goto S, Sato Y, Furumichi M, Tanabe M. KEGG for integration and interpretation of large-scale molecular data sets. Nucleic acids research. Oxford University Press; 2012;40:D109–14.

66. Caspi R, Billington R, Fulcher CA, Keseler IM, Kothari A, Krummenacker M, et al. The MetaCyc database of metabolic pathways and enzymes. Nucleic acids research. Oxford University Press; 2018;46:D633–9.

67. Yang C, Mai J, Cao X, Burberry A, Cominelli F, Zhang L. ggpicrust2: an R package for PICRUSt2 predicted functional profile analysis and visualization. Bioinformatics. Oxford University Press; 2023;39:btad470.

68. Louca S, Parfrey LW, Doebeli M. Decoupling function and taxonomy in the global ocean microbiome. Science. American Association for the Advancement of Science; 2016;353:1272–7.

69. Liu X, Chu H, Godoy O, Fan K, Gao G-F, Yang T, et al. Positive associations fuel soil biodiversity and ecological networks worldwide. Proceedings of the National Academy of Sciences. National Academy of Sciences; 2024;121:e2308769121.

70. Che J, Wu Y, Yang H, Wang S, Wu W, Lyu L, et al. Root niches of Blueberry Imprint increasing bacterial-fungal interkingdom interactions along the Soil-Rhizosphere-Root Continuum. Microbiology spectrum. American Society for Microbiology 1752 N St., NW, Washington, DC; 2023;11:e05333-22.

71. Li J, Huang X, Li S, Tang R, Su J. Microbial network complexity and diversity together drive the soil ecosystem multifunctionality of forests during different woodland use intensity in dry and wet season. Forest Ecology and Management. Elsevier; 2023;542:121086.

72. Fan M, Li J, Luan X, Yang L, Chen W, Ma X, et al. Biogeographical patterns of rhizosphere microbial communities in Robinia pseudoacacia forests along a north–south transect in the Loess Plateau. Geoderma. Elsevier; 2023;435:116516.

73. Fitzpatrick CR, Copeland J, Wang PW, Guttman DS, Kotanen PM, Johnson MT. Assembly and ecological function of the root microbiome across angiosperm plant species. Proceedings of the National Academy of Sciences. National Academy of Sciences; 2018;115:E1157–65.

74. Zannier, F., Portero, L. R., Douki, T., Gärtner, W., Farías, M. E., & Albarracín, V. H. (2022). Proteomic signatures of microbial adaptation to the highest ultraviolet-irradiation on earth: Lessons from a soil actinobacterium. Frontiers in Microbiology, 13, 791714.

75. Gtari, M., Essoussi, I., Maaoui, R., Sghaier, H., Boujmil, R., Gury, J., ... & Normand, P. (2012). Contrasted resistance of stone-dwelling Geodermatophilaceae species to stresses known to give rise to reactive oxygen species. FEMS Microbiology Ecology, 80(3), 566-577.

76. Lareen A, Burton F, Schäfer P. Plant root-microbe communication in shaping root microbiomes. Plant molecular biology. Springer; 2016;90:575–87.

77. Liu S, Wang T, Lu Q, Li F, Wu G, Jiang Z, et al. Bioprospecting of soil-derived Actinomycetota along the Alar-Hotan desert highway in the Taklamakan desert. Frontiers in Microbiology. Frontiers Media SA; 2021;12:604999.

78. Zheng Q, Hu Y, Kosina SM, Van Goethem MW, Tringe SG, Bowen BP, et al. Conservation of beneficial microbes between the rhizosphere and the cyanosphere. New Phytologist. Wiley Online Library; 2023;240:1246–58.

79. Li N, Liu R, Chen J, Wang J, Hou L, Zhou Y. Enhanced phytoremediation of PAHs and cadmium contaminated soils by a Mycobacterium. Science of the Total Environment. Elsevier; 2021;754:141198.

80. Mousa WK, Abu-Izneid T, Salah-Tantawy A. High-throughput sequencing reveals the structure and metabolic resilience of desert microbiome confronting climate change. Frontiers in Plant Science. Frontiers Media SA; 2024;15:1294173.

81. Sbissi I, Chouikhi F, Ghodhbane-Gtari F, Gtari M. Ecogenomic insights into the resilience of keystone Blastococcus Species in extreme environments: a comprehensive analysis. BMC genomics. Springer; 2025;26:51.

82. Tang K, Liang Y, Yuan B, Meng J, Feng F. Spatial distribution and core community of diazotrophs in Biological soil crusts and subsoils in temperate semi-arid and arid deserts of China. Frontiers in Microbiology. Frontiers Media SA; 2023;14:1074855.

83. Moisander PH, McClinton Iii E, Paerl HW. Salinity effects on growth, photosynthetic parameters, and nitrogenase activity in estuarine planktonic Cyanobacteriota. Microbial ecology. JSTOR; 2002;432–42.

84. Liu F, Li J, Feng G, Li Z. New genomic insights into “Entotheonella” symbionts in Theonella swinhoei: Mixotrophy, anaerobic adaptation, resilience, and interaction. Frontiers in microbiology. Frontiers Media SA; 2016;7:1333.

85. Starke R, Bastida F, Abadía J, García C, Nicolás E, Jehmlich N. Ecological and functional adaptations to water management in a semiarid agroecosystem: a soil metaproteomics approach. Scientific reports. Nature Publishing Group UK London; 2017;7:10221.

86. Acuña JJ, Campos M, de la Luz Mora M, Jaisi DP, Jorquera MA. ACCD-producing rhizobacteria from an Andean Altiplano native plant (Parastrephia quadrangularis) and their

potential to alleviate salt stress in wheat seedlings. Applied soil ecology. Elsevier; 2019;136:184–90.

87. Dong F, Wang L, Xu T, Yan Q, Yan S, Li F, et al. Multi-omics analysis of soil microbiota and metabolites in dryland wheat fields under different tillage methods. Scientific Reports. Nature Publishing Group UK London; 2024;14:24066.

88. Tuong HM, Méndez SG, Vandecasteele M, Willems A, Iancheva A, Ngoc PB, et al. A novel Microbacterium strain SRS2 promotes the growth of Arabidopsis and MicroTom (S. lycopersicum) under normal and salt stress conditions. Planta. Springer; 2024;260:79.

89. Astuti AFRS, Widyastuti R, Yusuf SM. Use of Sphingomonas yunannensis to Improve Soil Drought Stress in Chili Plants. Jurnal Ilmu Pertanian Indonesia. 2025;30:195–203.

90. Wang Y, Peng B, Zhao S, Zhou J, Tian C. Salinity stress reveals keystone metabolites linking rhizosphere metabolomes and microbiomes in Halophyte Suaeda salsa. Plant and Soil. Springer; 2025;1–21.

91. Albuquerque, L., Simoes, C., Nobre, M. F., Pino, N. M., Battista, J. R., Silva, M. T., ... & de Costa, M. S. (2005). Truepera radiovictrix gen. nov., sp. nov., a new radiation resistant species and the proposal of Trueperaceae fam. nov. FEMS microbiology letters, 247(2), 161-169.

92. Sorouri, B., Rodriguez, C. I., Gaut, B. S., & Allison, S. D. (2023). Variation in Sphingomonas traits across habitats and phylogenetic clades. Front Microbiol 14: 1146165.

93. Shu X, Liu W, Hu Y, Xia L, Fan K, Zhang Y, et al. Ecosystem multifunctionality and soil microbial communities in response to ecological restoration in an alpine degraded grassland. Frontiers in Plant Science. Frontiers Media SA; 2023;14:1173962.

94. Castro-Severyn J, Pardo-Esté C, Mendez KN, Fortt J, Marquez S, Molina F, et al. Living to the high extreme: unraveling the composition, structure, and functional insights of bacterial communities thriving in the arsenic-rich Salar de Huasco altiplanic ecosystem. Microbiology spectrum. American Society for Microbiology 1752 N St., NW, Washington, DC; 2021;9:10.1128/spectrum. 00444-21.

95. Tripathi BM, Kim M, Singh D, Lee-Cruz L, Lai-Hoe A, Ainuddin AN, et al. Tropical soil bacterial communities in Malaysia: pH dominates in the equatorial tropics too. Microbial ecology. Springer; 2012;64:474–84.

96. Lin Y, Ye Y, Hu Y, Shi H. The variation in microbial community structure under different heavy metal contamination levels in paddy soils. Ecotoxicology and environmental safety. Elsevier; 2019;180:557–64.

97. Bulgarelli D, Schlaeppi K, Spaepen S, Van Themaat EVL, Schulze-Lefert P. Structure and functions of the bacterial microbiota of plants. Annual review of plant biology. Annual Reviews; 2013;64:807–38.

98. Panchal, P., Preece, C., Peñuelas, J., & Giri, J. (2022). Soil carbon sequestration by root exudates. Trends in Plant Science, 27(8), 749-757.

99. Kuzyakov, Y., & Xu, X. (2013). Competition between roots and microorganisms for nitrogen: mechanisms and ecological relevance. New Phytologist, 198(3), 656-669.

100. Sun, H., Zhou, Y., & Jiang, C. (2024). Regulating denitrification in constructed wetlands: the synergistic role of radial oxygen loss and root exudates. Water, 16(24), 3706.

101. Torregrosa-Crespo, J., Miralles-Robledillo, J. M., Bernabeu, E., Pire, C., & Martínez-Espinosa, R. M. (2023). Denitrification in hypersaline and coastal environments. FEMS Microbiology Letters, 370, fnad066.

102. Roothans, N., Gabriëls, M., Abeel, T., Pabst, M., van Loosdrecht, M. C., & Laureni, M. (2024). Aerobic denitrification as an N2O source from microbial communities. The ISME journal, 18(1), wrae116.

103. Gamit, H., & Amaresan, N. (2023). Role of methylotrophic bacteria in managing abiotic stresses for enhancing agricultural production. Pedosphere, 33(1), 49-60.

104. Tang, H., Shi, L., Wen, L., Cheng, K., Sun, M., Sun, G., ... & Guo, Y. (2024). Effects of different long-term fertilization on rhizosphere soil nitrogen mineralization and microbial community composition under the double-cropping rice field. Archives of Agronomy and Soil Science, 70(1), 1-16.

105. Goszcz, A., Furtak, K., Stasiuk, R., Wójtowicz, J., Musiałowski, M., Schiavon, M., & Dębiec-Andrzejewska, K. (2025). Bacterial osmoprotectants—a way to survive in saline conditions and potential crop allies. FEMS Microbiology Reviews, 49, fuaf020.

106. Reumann, S. (2013). Biosynthesis of vitamin K1 (phylloquinone) by plant peroxisomes and its integration into signaling molecule synthesis pathways. Peroxisomes and their key role in cellular signaling and metabolism, 213-229.

107. Shahid, M., Singh, U. B., Khan, M. S., Singh, P., Kumar, R., Singh, R. N., ... & Singh, H. V. (2023). Bacterial ACC deaminase: Insights into enzymology, biochemistry, genetics, and potential role in amelioration of environmental stress in crop plants. Frontiers in microbiology, 14, 1132770.

108. Gahan, J., & Schmalenberger, A. (2014). The role of bacteria and mycorrhiza in plant sulfur supply. Frontiers in plant science, 5, 723.

109. Chaudhary, S., Sindhu, S. S., Dhanker, R., & Kumari, A. (2023). Microbes-mediated sulphur cycling in soil: Impact on soil fertility, crop production and environmental sustainability. Microbiological research, 271, 127340.